THE JOURNAL OF PHYSICAL CHEMISTRY B

A JOURNAL OF THE AMERICAN CHEMICAL SOCIETY

June 23, 2022
Volume 126
Number 24
pubs.acs.org/JPCB

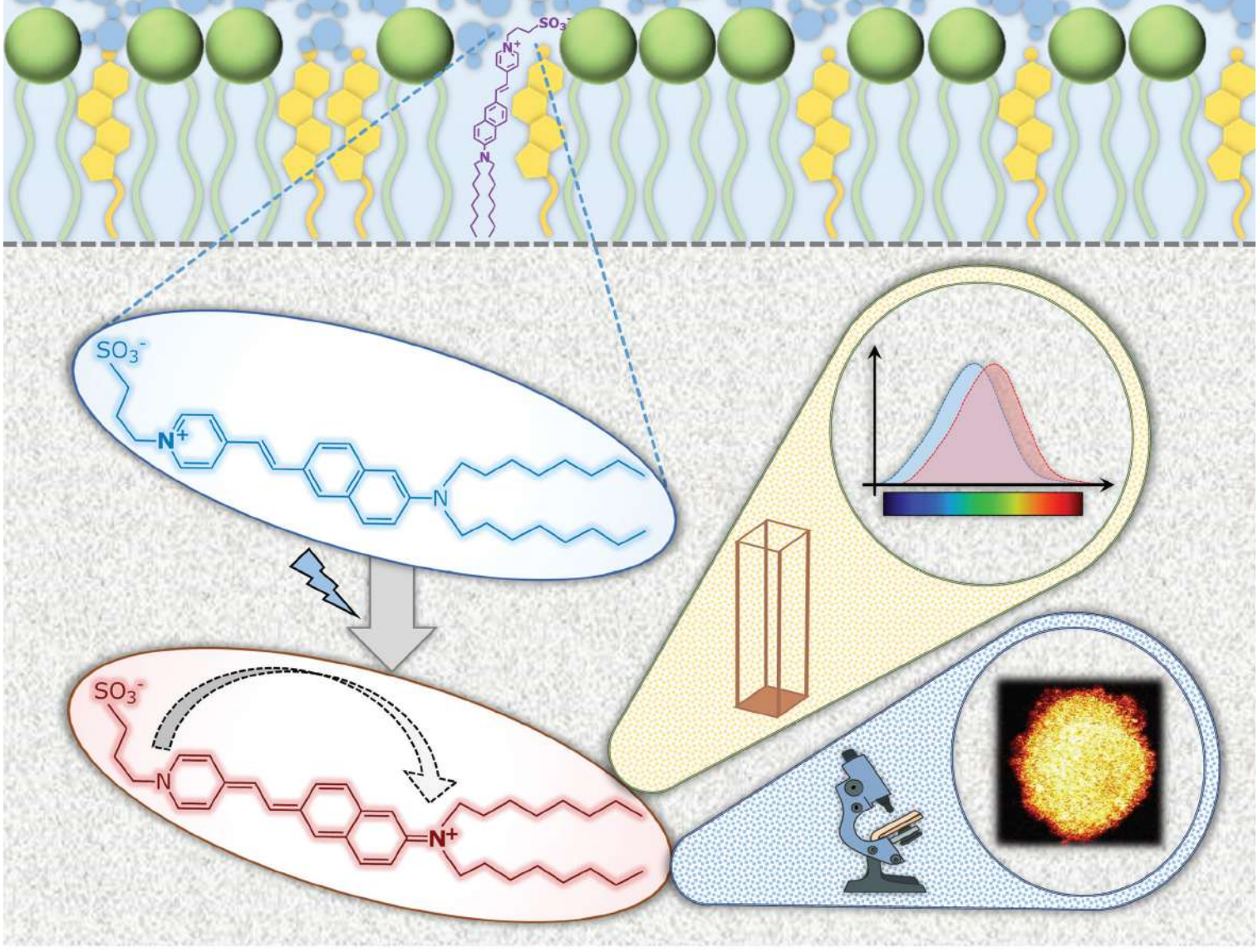

ACS Publications
Most Trusted. Most Cited. Most Read.

www.acs.org

THE JOURNAL OF PHYSICAL CHEMISTRY B
A JOURNAL OF THE AMERICAN CHEMICAL SOCIETY

pubs.acs.org/JPCB

Feature Article

Membrane Dipole Potential: An Emerging Approach to Explore Membrane Organization and Function

Parijat Sarkar and Amitabha Chattopadhyay*

Cite This: *J. Phys. Chem. B* 2022, 126, 4415−4430

Read Online

ACCESS | Metrics & More | Article Recommendations

ABSTRACT: Biological membranes are complex organized molecular assemblies of lipids and proteins that provide cells and membrane-bound intracellular organelles their individual identities by morphological compartmentalization. Membrane dipole potential originates from the electrostatic potential difference *within* the membrane due to the nonrandom arrangement (orientation) of amphiphile and solvent (water) dipoles at the membrane interface. In this Feature Article, we will focus on the measurement of dipole potential using electrochromic fluorescent probes and highlight interesting applications. In addition, we will focus on ratiometric fluorescence microscopic imaging technique to measure dipole potential in cellular membranes, a technique that can be used to address novel problems in cell biology which are otherwise difficult to address using available approaches. We envision that membrane dipole potential could turn out to be a convenient tool in exploring the complex interplay between membrane lipids and proteins and could provide novel insights in membrane organization and function.

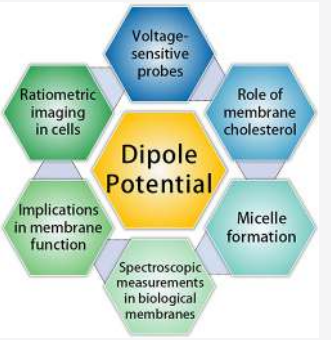

THE MOLECULAR ORIGIN OF MEMBRANE DIPOLE POTENTIAL

Biological membranes are quasi-two-dimensional thin sheets of lipid bilayers of ∼5 nm thickness comprising a diverse array of lipids and proteins held together by noncovalent interactions. Biomembranes act as a semipermeable barrier for ions, proteins, and other macromolecules, which separates the cellular interior from the extracellular milieu and provide the cell its unique identity.[1] To overcome this selective barrier, specialized membrane proteins such as ion channels, carriers, and pumps are embedded in the membrane that allow selective transport of materials across the lipid bilayer. As a result of the selective barrier properties of membranes, concentrations of ions on both sides of membranes (intracellular vs extracellular) are drastically different, leading to generation of an electrical potential difference due to an imbalance of charge across the membrane. This is defined as the transmembrane potential (represented as Ψ in Figure 1a). The magnitude of Ψ is in the range of 10−100 mV in cells[3,4] and is an important regulator of the function of membrane proteins such as voltage-gated ion channels.[5] Transmembrane potential is relatively easy to measure by placing electrodes on both sides of the membrane. On the other hand, the surface potential (denoted as Ψ_S) arises due to charged headgroups of lipid molecules and adsorbed ions at the surface of the membrane. The surface potential decays exponentially away from the membrane surface and could be calculated using the Gouy−Chapman model.[6]

The membrane dipole potential, Ψ_d, is an electrical potential difference *within* the membrane that drops across the lipid headgoup region of a lipid bilayer (Figure 1a).[7−9] The origin of Ψ_d lies in the anisotropic (nonrandom) arrangement of lipid and water dipoles at the membrane interface giving rise to a net electrical field within the membrane. The major contributor to the magnitude of dipole potential is oriented water dipoles that form hydrogen bonds with the carbonyl oxygen in the ester linkage between the glycerol backbone and the *sn*-2 hydrocarbon chain of phospholipids.[10−14] Importantly, the chemical nature of phospholipid headgroup is believed to be another factor that could modulate the magnitude of Ψ_d.[13] However, in case of the phosphatidylcholine (PC) headgroup, the major phospholipid species in higher eukaryotic membranes, the P^-−N^+ dipole between the phosphate group and nitrogen of the choline headgroup is not a major contributing factor of Ψ_d, since it is thought to lie parallel to the membrane surface.[14] Interestingly, polyunsaturated fatty acids (PUFAs) could influence the magnitude of dipole potential.[15] The existence of dipole potential was discovered in 1969 by two Russian scientists, Liberman and Toplay,[16] during their work on carrier mechanism of fat-soluble (hydrophobic) tetraphenylborate (TPB^-) and tetraphenylphosphonium (TPP^+) ions across lipid membranes (see Figure 1b for chemical structures). Their results revealed that membrane conductivity was $\sim 10^5$ times higher with TPB^- than with TPP^+, although both ions have identical radii. They hypothesized that the difference in

Received: April 11, 2022
Revised: May 21, 2022
Published: June 13, 2022

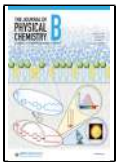

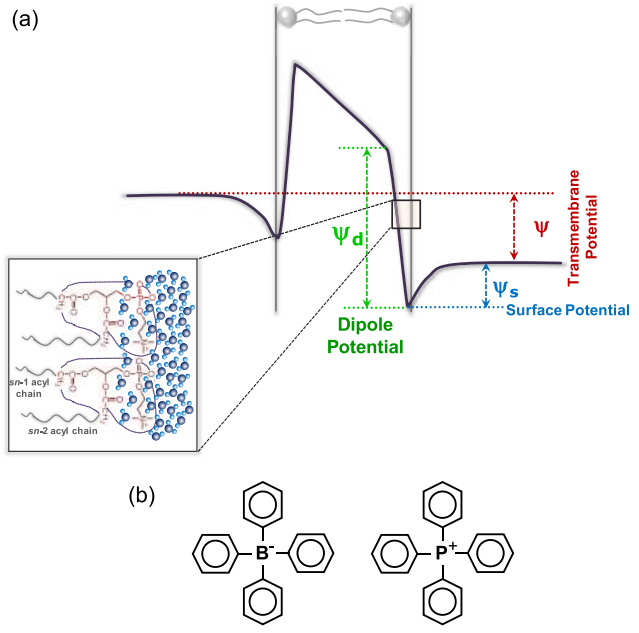

Figure 1. (a) A schematic representation of electrostatic potentials associated with biomembranes. The transmembrane potential (Ψ) arises due to the net separation of charges between the two bulk aqueous phases across the membrane. The surface potential (Ψ_S) is the potential difference between the membrane surface and the bulk aqueous phase and arises from charged molecules that are associated with the membrane−water interface. The dipole potential (represented as Ψ_d) is attributed to the potential difference that arises due to the nonrandom orientation of dipolar residues of the lipids and associated water molecules within the membrane. Reprinted with permission from ref 2. Copyright 1994 Elsevier; see ref 2 for more details. (b) Chemical structures of representative hydrophobic ions tetraphenylborate (TPB^-) and triphenylphosphonium (TPP^+).

membrane conductivity is due to an energy barrier within the membrane *due to presence of a positive potential within the membrane*. The term dipole potential and the concept of oriented molecular dipoles inside the membrane were first used by Hladky and Haydon in their work on specific conductance of artificial planar membranes of PC, cholesterol, and glycerol monooleate.[17]

METHODS FOR MEASUREMENT OF MEMBRANE DIPOLE POTENTIAL

Although the concept of membrane dipole potential has its origins in the 1970s, its application in the area of membrane biology and biophysics has been slow, due to lack of suitable experimental approaches for its measurement.[18,19] Dipole potential is difficult to measure since the potential difference lies within the membrane and drops over a distance of a few angstroms.[2] Depending on the lipid composition, Ψ_d has been estimated to be in the range of 100−1000 mV, which would be expected to produce an electric field strength of $\sim 10^8-10^9$ V m^{-1}.[8,20] Dipole potential in membranes and other organized molecular assemblies is popularly measured by a ratiometric fluorescence approach using voltage-sensitive fluorophores, initially developed by Leslie Loew.[2,21−29] The mechanism underlying the voltage sensitivity of these probes is electrochromic in nature which involves a large movement of electronic charge within the molecule when it is excited from the ground state to the excited state (Figure 2a). In such a scenario, if the direction of the movement of charge lies parallel to an electric

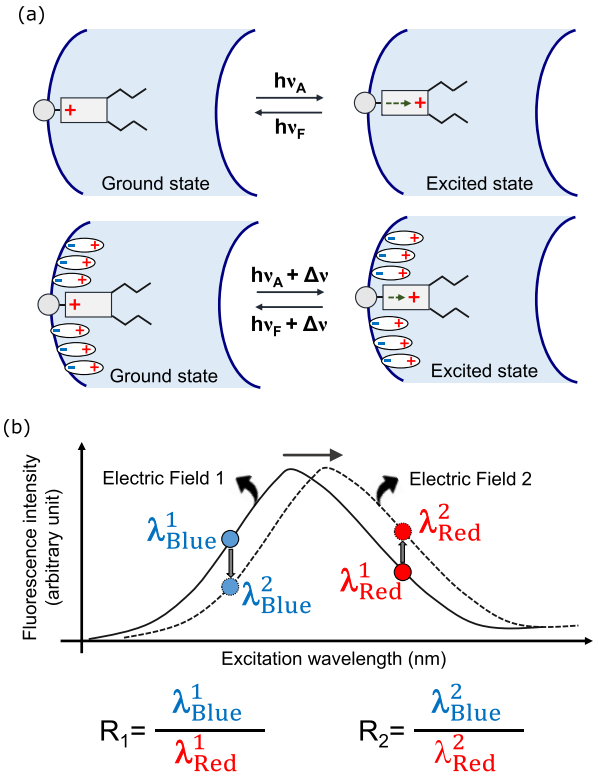

Figure 2. (a) Representation of a charge-shift probe bound to the membrane and the origin of its response to a change in membrane potential. The fluorophore, represented by the rectangle, is anchored perpendicular to the membrane surface as a result of a polar group at one end (represented by a circle) and hydrocarbon chains (represented by a zigzag) on the other end. Excitation from the ground state to the first excited state causes a large shift in charge down the long axis of the chromophore (top panel). When the direction of the charge movement lies parallel to an electric field (such as the field generated due to the membrane dipole potential), membrane potential modulates this charge redistribution (shown in the bottom panel) and alters the excitation ($h\nu_A$) or emission ($h\nu_F$) energies. Reprinted with permission from ref 24. Copyright 1982 Elsevier; see ref 24 for more details. (b) A schematic representation of fluorescence excitation spectra of electrochromic probes in the presence of varying electric fields. The shift in the excitation spectrum of styryl probes is associated with the local electric field strength, the mechanism being electrochromic in nature. The fluorescence intensity ratio (R), defined as the ratio of fluorescence intensity values at the blue edge (λ_{Blue}) and red edge (λ_{Red}) of the spectrum, is proportional to the dipole potential value of the membrane. Since R is calculated as a ratio of fluorescence intensities, dipole potential could be measured regardless of uneven probe distribution.

field (such as the dipolar field within the membrane), the transition energy would be sensitive to the strength of the external electric field. If the fluorophore in an electrochromic probe is oriented in such a way that the charge redistribution is perpendicular to the membrane surface, it can be used as a good indicator of membrane dipole potential. A change in dipole potential will change the energy needed to excite the chromophore and would be reflected in its fluorescence spectra which can be experimentally recorded (see Figure 2b). As a result, the excitation spectrum undergoes a shift due to a change in the electric field where the probe is localized (shown in Figure 2b). The fluorescence intensity decreases on the blue edge of the spectrum and shows an increase in the red edge due to decrease in electric field. A ratio of fluorescence intensities at two wavelengths would therefore represent a measure of the probe's

https://doi.org/10.1021/acs.jpcb.2c02476
J. Phys. Chem. B 2022, 126, 4415−4430

response to the electric field within the membrane. This ratio (defined as R) is a faithful indicator of the membrane dipole potential. Importantly, taking a ratio cancels out variations due to change in concentration of the probe as this would change the magnitude of fluorescence intensity in the same direction at both wavelengths. As a result, a fluorescence intensity ratio of the two wavelengths normalizes away other factors except the response of the dye to the electric field. Although the dual-wavelength fluorescence ratiometric approach using voltage-sensitive probes has emerged as the most popular approach to measure dipole potential, other experimental methods[8] such as electron spin resonance,[30] cryo-EM,[20] atomic force microscopy,[31] dielectric spectroscopy,[32] vibrational spectroscopy,[33−35] electrophysiology,[19] and molecular dynamics simulations[36−43] have been used for measurement of dipole potential.

USE OF VOLTAGE-SENSITIVE FLUORESCENT PROBES TO MEASURE DIPOLE POTENTIAL

Figure 3a shows representative examples of voltage-sensitive probes that are widely used for dipole potential measurements.

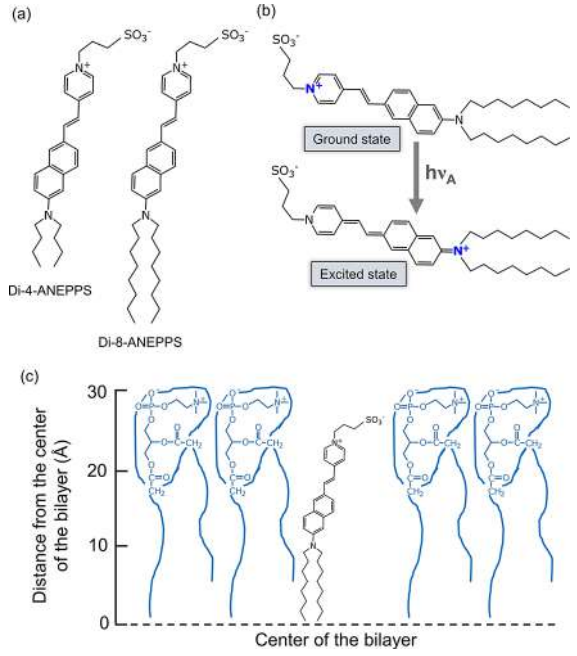

Figure 3. (a) Representative chemical structures of charge-shift styryl probes used for measuring membrane dipole potential. (b) Charge redistribution in electrochromic fluorophores upon excitation. The naphthylstyryl chromophore harbors a positive charge near the pyridinium nitrogen in the ground state. Upon excitation, the chromophore experiences a large charge redistribution and the positive charge is relocated near the arylamino nitrogen in the excited state. (c) The membrane location of the fluorescent styrylpyridinium group in di-8-ANEPPS is shown according to ref 44. The probe location is illustrated in between phosphatidylcholine lipids in the outer membrane leaflet. The horizontal dotted line at the bottom indicates the center of the bilayer. Reprinted with permission from ref 44. Copyright 2012 with Elsevier.

These probes belong to a structural class called styryl or naphthylstyryl dyes which are amphiphilic membrane labeling fluorophores that usually have a hydrophilic group acting as membrane anchor and two hydrocarbon chains that align the fluorophore parallel to the lipid molecules. The styryl probes that have been most popular include di-4-ANEPPS (4-(2-(6-(dibutylamino)-2-naphthalenyl)ethenyl)-1-(3-sulfopropyl)-pyridinium inner salt)[27,45] and di-8-ANEPPS (4-(2-(6-(dioctylamino)-2-naphthalenyl)ethenyl)-1-(3-sulfopropyl)-pyridinium inner salt)[2,46] (see Figure 3a). The naphthylstyryl chromophore harbors a positive charge near the pyridinium nitrogen in the ground state (as shown in Figure 3b).[21] Upon excitation, the chromophore experiences a large charge redistribution, and the positive charge is relocated near the arylamino nitrogen in the excited state (Figure 3b). Due to the presence of a hydrophilic moiety in one end and a pair of hydrocarbon chains to the other, the probe intercalates readily among the amphiphilic lipids in membranes (shown in Figure 3c). As a result, the chromophore is oriented perpendicular to the membrane surface which assures that the excitation-induced charge redistribution would take place parallel to the dipolar electric field within the membrane. A problem associated with di-4-ANEPPS is its rapid internalization in cells due to its short hydrocarbon tails. To overcome this, di-8-ANEPPS was synthesized in which the butyl chains were replaced with octyl chains.[2,46] Notably, using the Parallax method,[47] we previously reported that the depth of penetration of the fluorescent styrylpyridinium group, on the average, was ∼12.2 Å from the center of the bilayer (see Figure 3c).[44] This suggests that the fluorophore moiety in di-8-ANEPPS is localized at the interfacial region of the membrane, in agreement with its proposed interfacial localization.[2,48] Interestingly, the measured localization is consistent with the reported insensitivity of di-8-ANEPPS to surface potential.[2] It is worth mentioning that unlike the ratio of fluorescence intensities of the excitation spectrum of voltage-sensitive probes such as di-8-ANEPPS, the emission ratios do not correlate with the dipole potential in lipid vesicles.[49] Di-8-ANEPPS can therefore only be used via an excitation ratiometric mode to quantify the fluorescence intensity ratio (R) which is proportional to dipole potential. This is typically achieved by calculating the ratio of fluorescence intensities using excitation wavelengths at 420 and 520 nm with emission fixed at a red edge.[44,50−52] Although the absolute value of dipole potential has been difficult to measure, a linear relationship between R and Ψ_d is available in the literature as[51]

$$\Psi_d = (R + 0.3)/(4.3 \times 10^{-3}) \quad (1)$$

This is based on a calibration curve constructed using literature data of dipole potential from electrical measurements on monolayers and bilayers.[51] However, one must keep in mind that this relationship is based on measurements carried out in phosphatidylcholine vesicles and its extrapolation to other complex membranes is not straightforward.

Although fluorescence-based approaches have emerged as a useful tool to monitor dipole potential in biological membranes, they suffer from a few limitations[53] such as bleaching of probes during long-term experiments. Photobleaching could lead to undesirable photochemical activity (such as the production of reactive oxygen species or chemical reactivity with other membrane components) that could alter the chemical identity of the membrane. In addition, probes themselves could alter membrane physical properties if used at a higher lipid/probe ratio (see below).

Does the dipole of electrochromic probes such as di-8-ANEPPS contribute to the measured dipole potential? This is a relevant question and merits comment. It has been previously reported that di-8-ANEPPS could, in some cases, increase membrane dipole potential in a concentration-dependent manner.[50] However, in case of di-8-ANEPPS, it was observed

https://doi.org/10.1021/acs.jpcb.2c02476
J. Phys. Chem. B 2022, 126, 4415−4430

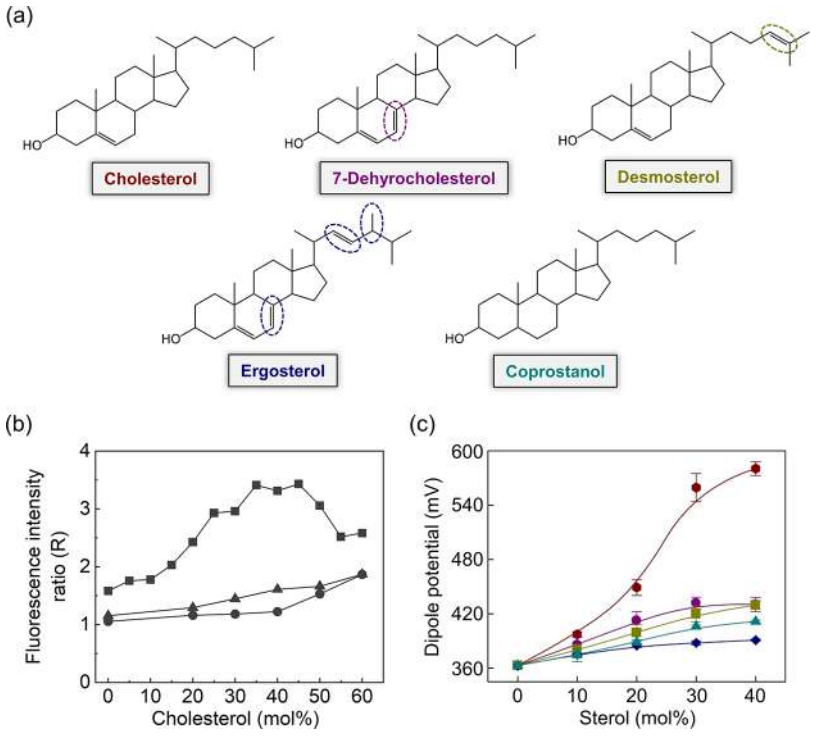

Figure 4. Cholesterol increases membrane dipole potential. (a) Chemical structures of cholesterol and its biosynthetic and evolutionary precursors. Cholesterol is an indispensable component of higher eukaryotic membranes and is the end product of a multistep sterol biosynthetic pathway. 7-DHC and desmosterol are immediate biosynthetic precursors of cholesterol in the Kandutsch−Russell and Bloch pathways, respectively. The chemical structure of 7-DHC differs with cholesterol only in an extra double bond at the 7th position in the sterol ring, and desmosterol differs with cholesterol only in an extra double bond at the 24th position in the alkyl side chain (highlighted in their respective structures). Ergosterol is the major sterol present in lower eukaryotes such as yeast and fungi. The chemical structure of ergosterol differs from that of cholesterol in two additional double bonds (at the 7th position in the sterol ring and the 22nd position in the alkyl side chain) and an additional methyl group at the 24th position in the alkyl side chain (highlighted). Coprostanol is a saturated sterol widely used as a biomarker. (b) Cholesterol increases the dipole potential of phosphatidylcholine vesicles. Fluorescence intensity ratio (R) measured using di-8-ANEPPS for DMPC (■), DOPC (▲), and egg PC (●) vesicles are shown. Lines joining the data points are provided merely as viewing guides. Reprinted with permission from ref 63. Copyright 2006 Elsevier; see ref 63 for more details. (c) Effect of sterols on dipole potential of membranes. Dipole potential in POPC membranes as a function of increasing concentrations of cholesterol (solid red hexagon), 7-DHC (solid purple circle), desmosterol (solid green square), ergosterol (solid blue triangle) and coprostanol (solid turquoise triangle) are shown. The effect of these precursors on membrane dipole potential is very different from that observed with cholesterol, although the structural differences among them are subtle. Lines joining the data points are provided merely as viewing guides. Reprinted with permission from ref 44. Copyright 2012 Elsevier; see ref 44 for more details.

that a molar excess of lipid molecules over dye of (i.e., at least 100-fold (lipid/dye, 100:1, mol/mol)) would circumvent any effect due to the dipole of the dye.[50] In other words, the plateauing nature of the change in dipole potential beyond 100:1 (mol/mol) ratio of lipid/di-8-ANEPPS represents a lower limit which is necessary to rule out any dye-induced artifacts. This essentially means that at probe concentrations of 1 mol % (or less), the dipole potential obtained will be free from the influence of the probe dipole.

■ ROLE OF CHOLESTEROL IN MODULATING DIPOLE POTENTIAL

Cholesterol is a crucial constituent of higher eukaryotic cellular membranes due to its central role in the organization and dynamics of the membrane and its functional implications in cellular physiology.[54−57] Cholesterol is nonrandomly organized into distinct domains on the cell membrane that serve as signaling hubs for biological functions. Apart from its indispensable role in maintaining the organization and structure of cell membranes,[58] cholesterol is implicated in essential cellular functions such as signal transduction and trafficking.[59] Due to its unique chemical structure (Figure 4a), cholesterol is known to influence several physicochemical properties of membranes. For example, cholesterol is known to modulate water penetration[60,61] and membrane thickness.[62] Using the di-8-ANEPPS dual-fluorescence ratiometric approach, Starke-Peterkovic et al. reported that 1,2-dimyristoyl-*sn*-glycero-3-phosphatidylcholine (DMPC) lipid vesicles containing increasing concentrations of cholesterol showed a progressive increase in dipole potential (Figure 4b).[63] They further showed that cholesterol could increase the dipole potential of both 1,2-dioleoyl-*sn*-glycero-3-phosphatidylcholine (DOPC, 18:1 PC) and egg PC (a mixture of 16:0, 18:0, 18:1, 18:2, and 20:4 PC), although the magnitude of the change is significantly smaller than that observed in DMPC (see Figure 4b). We showed that cholesterol induced a similar increase in dipole potential of 1-palmitoyl-2-oleoyl-*sn*-glycero-3-phosphophatidylcholine (POPC) membranes (Figure 4c).[44] The figure shows that the membrane dipole potential exhibited an increasing trend with increasing concentration of cholesterol and exhibited ∼60% increase relative to control POPC membranes (without cholesterol) in the presence of 40 mol % cholesterol.[44] These results are supported by previous observations that suggested cholesterol increases dipole potential in monoolein bilayer[64] and egg PC monolayer[65] and recent observations made with

https://doi.org/10.1021/acs.jpcb.2c02476
J. Phys. Chem. B 2022, 126, 4415−4430

molecular dynamics simulation,[38,39] dielectric spectroscopy[32] vibrational spectroscopy,[35] and fluorescence spectrocopy.[66] The ability of cholesterol to increase the dipole potential of membranes could emanate from its unique molecular attributes such as dipole moment perpendicular to the membrane surface or through cholesterol induced changes on membrane organization (e.g., condensation of lipid headgroup area and/or water penetration).[63] In addition, a combination of both these effects could be operative.[63]

In higher eukaryotes, cholesterol is synthesized as the end product of a long, multistep and highly regulated process that involves more than 20 enzymes. Cholesterol is synthesized via desmosterol (the Bloch pathway) or 7-dehydrocholesterol (7-DHC, the Kandutsch−Russel pathway) as immediate biosynthetic precursors.[67,68] The differences in chemical structure between cholesterol and its immediate biosynthetic precursors are subtle. Whereas 7-DHC differs with cholesterol only by a double bond at the 7th position in the fused steroid ring, desmosterol has only an additional double bond at the 24th position in its alkyl side chain (see Figure 4a). The relative contributions of these two pathways are stringently controlled depending on tissue-type and age.[69] Interestingly, the accumulation of cholesterol biosynthetic precursors is implicated in severe pathophysiological conditions.[70,71] For example, accumulation of 7-DHC is associated with Smith−Lemli−Opitz syndrome, a manifestation of defective cholesterol biosynthesis that results in growth impairment and mental retardation.[72−75] In terms of the evolution of sterol structures, ergosterol represents an important evolutionary precursor of cholesterol and is the major sterol found in lower eukaryotes such as protozoa, fungi, yeast, and insects such as Drosophila.[76] The chemical structure of ergosterol differs from that of cholesterol in two additional double bonds (at 7th and 22nd positions) and an extra methyl group at the 24th position of the side chain (see Figure 4a). Do biosynthetic and evolutionary precursors of cholesterol induce a similar dipolar environment in the membrane as observed with cholesterol? Notably, the two immediate biosynthetic precursors of cholesterol, 7-DHC and desmosterol, display a relatively modest increase in dipole potential up to ∼430 mV at the highest sterol concentration (increase of ∼18% in both cases, Figure 4c).[44] The increase in dipole potential was even less (∼8%) when ergosterol was used. As a control, we measured dipole potential with coprostanol (a saturated sterol with no double bond used as a biomarker) which exhibited ∼13% increase in dipole potential with its highest concentration (Figure 4c).[44] Although it has been previously shown that these sterols, which differ with cholesterol only subtly, exert differential effects on membrane organization,[77−81] the differential effect on dipole potential merits comment. Membrane dipole potential (Ψ_d) is related to dipole moment (μ) and dielectric constant (ε) of the medium according to the Helmholtz equation:[8]

$$\Psi_d = \mu_\perp/(A\varepsilon_0\varepsilon) \quad (2)$$

where $\mu_\perp$ is the perpendicular component of dipole moment along the bilayer normal, A is the area per lipid molecule, and ε_0 is the permittivity in vacuum. According to this relationship, dipole potential should vary inversely with the effective molecular area[8] and linearly with dipole moment. A lower value of membrane dipole potential in the presence of 7-DHC could be attributed to the lower dipole moment of 7-DHC (1.42 D) relative to cholesterol (1.87 D) possibly due to shortening of bond length and difference in tilt angle in the membrane.[44] In addition, the headgroup area of a lipid molecule in the membrane bilayer has been reported to be greater in the presence of 7-DHC (or desmosterol) relative to cholesterol.[80,82] This implies that due to the difference in the condensing ability of these sterols, dipole density is less in the presence of 7-DHC (or desmosterol), which could lead to a reduction in dipole potential. Overall, these results point out that the ability of a sterol to modulate membrane dipole potential is varied and depends on its molecular structure. Notably, even a subtle difference in the chemical structure (such as an additional double bond) could give rise to a drastic difference in their ability to modulate dipole potential.

Cholesterol plays a crucial role in the cellular function of membrane proteins and receptors owing to its unique structural and stereochemical features.[83−86] Stereoisomers of cholesterol such as *ent*-cholesterol (enantiomer of cholesterol) and *epi*-cholesterol (diastereomer of cholesterol) have been used as useful tools to discriminate between specific and general effects of cholesterol in membrane protein function (Figure 5a).[85−91] Whereas *ent*-cholesterol is a nonsuperimposable mirror image of natural cholesterol and has identical physicochemical properties (such as compressibility and phase behavior) except for the direction of rotation of plane-polarized light,[88,92−94] *epi*-cholesterol is a diastereomer of cholesterol in which only the

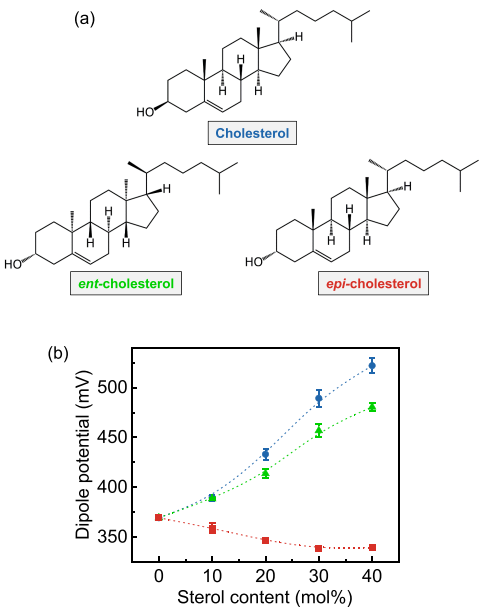

Figure 5. Membrane dipole potential is sensitive to cholesterol stereospecificity. (a) Chemical structures of cholesterol, *ent*-cholesterol and *epi*-cholesterol. Both *ent*-cholesterol and *epi*-cholesterol are stereoisomers of cholesterol. *ent*-Cholesterol is the enantiomer of cholesterol (enantiomers are nonsuperimposable mirror images of one another). *epi*-Cholesterol, on the other hand, is a diastereomer and is not a mirror image of cholesterol. *ent*-Cholesterol (but not *epi*-cholesterol) shares identical physicochemical properties with cholesterol. (b) Dipole potential in POPC membranes with increasing concentrations of cholesterol (solid blue circle), *ent*-cholesterol (solid green triangle), and *epi*-cholesterol (solid red square). Both cholesterol and *ent*-cholesterol share comparable ability in increasing membrane dipole potential. In contrast, *epi*-cholesterol displays a reduction in membrane dipole potential and lacks the ability to increase dipole potential. Lines joining the data points are provided merely as viewing guides. Reprinted with permission from ref 97. Copyright 2014 Elsevier; see ref 97 for more details.

https://doi.org/10.1021/acs.jpcb.2c02476
J. Phys. Chem. B 2022, 126, 4415−4430

orientation of the hydroxyl group is inverted relative to native cholesterol (Figure 5a). As a result, the biophysical properties (such as tilt angles, condensing ability, and phase transition) of *epi*-cholesterol and native cholesterol are different.[88,94−96] We previously showed that *ent*-cholesterol and cholesterol share comparable ability in increasing membrane dipole potential (Figure 5b).[97] In contrast, the change in membrane dipole potential is drastically different for *epi*-cholesterol and cholesterol. Our results showed that not only *epi*-cholesterol is unable to increase membrane dipole potential but also there is a slight reduction in membrane dipole potential with increasing concentrations of *epi*-cholesterol (see Figure 5b).[97] It has been previously reported that *ent*-cholesterol, but not *epi*-cholesterol, could replace normal cholesterol in supporting normal growth of mammalian cell lines[98,99] and function of GPCRs.[91] These results suggest that dipole potential is sensitive to subtle changes in sterol structures and this could be used as a useful tool to monitor altered lipid−protein interactions due to subtle changes in lipid structure.

FUNCTIONAL IMPLICATIONS OF MEMBRANE DIPOLE POTENTIAL

It is natural that dipole potential would play a crucial functional role in membranes since the electric field generated by dipole potential is $\sim 10^8-10^9$ V m^{-1}, which is at least 1 order of magnitude higher than the field strength generated by a 100 mV of transmembrane potential ($\sim 2.5 \times 10^7$ V m^{-1}).[9] Membrane dipole potential is known to influence the translocation rates of ions across lipid membranes[100] and partition and translocation of larger molecules.[101,102] Importantly, dipole potential is known to influence the structure and function of membrane proteins, such as the Na^+-K^+-ATPase,[51] phospholipase A_2,[103] the ion channel gramicidin,[37,104−106] the simian immunodeficiency viral fusion peptide,[107] receptor tyrosine kinases,[108] and amphiphilic peptides such as p25.[109] Table 1 shows a comprehensive list of membrane proteins (and peptides) whose functions are known to be affected by a change in membrane dipole potential. In addition, dipole potential is sensitive to interaction of proteins with membrane.[109,125,126] Interestingly, the action of anesthetics has been shown to be via modulation of membrane dipole potential.[106,127−133] It has also been suggested that local dipole potential could play an important role in the function of proteins localized to specialized membrane microdomains, where the dipole potential is different from the bulk membrane due to the enrichment of cholesterol in these domains.[134,135]

We extended dipole potential measurements to complex natural membranes such as the bovine hippocampal membrane and explored the functional correlates between dipole potential and receptor activity. For this, we monitored the ligand binding function of the serotonin$_{1A}$ receptor, a neurotransmitter receptor in the G protein-coupled receptor (GPCR) superfamily,[136−139] and explored receptor−cholesterol interaction by dipole potential measurements. Figure 6a shows the dipole potential of hippocampal membranes measured utilizing the voltage-sensitive probe di-8-ANEPPS with increasing cholesterol depletion.[140] The figure shows that the dipole potential of native hippocampal membranes displays progressive reduction with decreasing membrane cholesterol content (i.e., with increasing cholesterol depletion). This is in overall agreement with previous reports in which it was shown that cholesterol increases membrane dipole potential.[44,63] In addition, we previously showed that the polarity (as measured by dielectric constant) of hippocampal membranes increases upon cholesterol depletion.[141] The observed reduction in dipole potential values in cholesterol-depleted hippocampal membranes could be attributed to the increase in the dielectric constant, since dipole potential is inversely related to the dielectric constant (see eq 2).[8,44,63] Figure 6a further highlights the relevance of membrane dipole potential in the context of the activity of the serotonin$_{1A}$ receptor, as measured by specific radiolabeled agonist ([^{3}H]8-OH-DPAT) binding. The strong correlation observed between change in receptor activity and membrane dipole potential under cholesterol-depleted conditions is noteworthy (Figure 6a). We further showed that replenishment with 7-DHC in cholesterol-depleted hippocampal membranes

Table 1. List of Membrane Proteins and Peptides Whose Functions Are Sensitive to Dipole Potential

protein/peptide	affected function	ref
p25 (amphipathic signal sequence of subunit IV of cytochrome *c* oxidase)	• membrane insertion and folding	109
	• binding affinity	36
gramicidin A	• open channel lifetime	104
	• proton conductance	37, 105
	• channel conductance	106
simian immunodeficiency virus fusion peptide (12 residue N-terminal segment of gp32)	membrane fusion	107
Na^+-K^+-ATPase	ATPase activity	51
antibiotic peptide bacitracin	skin permeability	110
human immunodeficiency virus protease inhibitor saquinavir	membrane binding	111
phospholipase A_2	degradation of phospholipids	103
syringomycin E	• channel conductance, lifetime, and number of synchronously operating small channels in the clusters	112
	• channel-forming activity	113
	• pore-forming activity	114
surfactin	membrane conductance	115
ErB	clustering and ligand binding affinity	108, 116
alamethicin	• channel-forming activity	117, 118
	• binding affinity	36
	• peptide orientation	119
WALP23	binding affinity	36
HIV fusion peptide gp41	binding affinity	36, 120
magainin	binding affinity	36
cecropins	channel-forming activity	121
P-glycoprotein	ligand binding	122
signal sequence of *E. coli* LamB	membrane interaction	123
penetratin	• endolysosomal entry	115
	• cell penetration	124

https://doi.org/10.1021/acs.jpcb.2c02476
J. Phys. Chem. B 2022, 126, 4415−4430

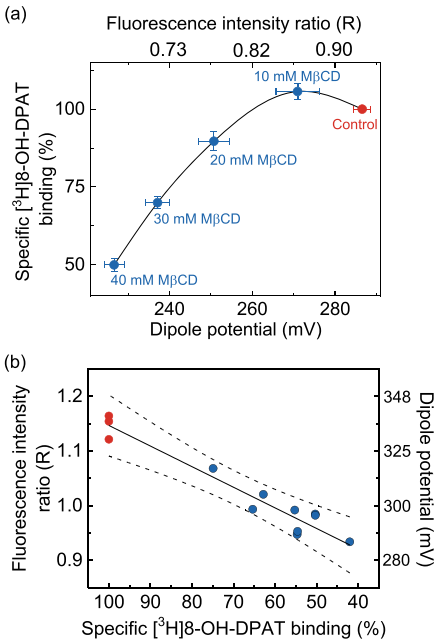

Figure 6. Influence of dipole potential on ligand binding activity of serotonin$_{1A}$ receptors in hippocampal membranes. (a) Specific [^{3}H]8-OH-DPAT (agonist) binding to serotonin$_{1A}$ receptors are plotted against the corresponding dipole potential in hippocampal membranes. Cholesterol content in hippocampal membranes was depleted using treatment with increasing concentrations of methyl-β-cyclodextrin (MβCD). Reprinted with permission from ref 140. Copyright 2012 Elsevier; see ref 140 for more details. (b) Correlation of specific agonist binding activity of the serotonin$_{1A}$ receptor with membrane dipole potential upon solubilization. Every data point represents measurements of specific [^{3}H]8-OH-DPAT binding and the corresponding value of membrane dipole potential. Linear regression analysis yielded a correlation coefficient of ~0.96. The significance of the correlation is apparent from the 99% confidence band (plotted as dashed lines). The influence of membrane dipole potential on the activity of the serotonin$_{1A}$ receptor is noteworthy. Reprinted with permission from ref 144. Copyright 2017 Elsevier; see ref 144 for more details.

could not restore the ligand binding activity of the serotonin$_{1A}$ receptor.[140] This is attributed to the inability of 7-DHC in restoring the dipole potential in hippocampal membranes (see Figure 4c).[44,140] As discussed earlier, a lower value of membrane dipole potential in the presence of 7-DHC could be attributed to the lower dipole moment of 7-DHC relative to cholesterol.[44] In addition, the inability of 7-DHC to support receptor function could be further due to the differential ability of cholesterol and 7-DHC to polarize water molecules at the membrane interface.[63,142] These results suggest that the cooperative interplay between membrane lipids and proteins that manifests in functional changes of membrane proteins could be interpreted using membrane dipole potential as a sensitive readout. For example, the inhibition of the activity of Na^+-K^+-ATPase by ether lipids[143] could be due to the larger dipole potential for ester lipid membranes than ether lipid membranes.[11,20]

We further explored the usefulness of membrane dipole potential measurement as an indicator of membrane protein solubilization.[144] Solubilization of membrane proteins by detergents represents a critical step in the purification of membrane proteins.[85,145,146] Solubilization leads to dissociation of proteins and lipids from natural membranes into mixed clusters of lipids, proteins, and micelles in the aqueous dispersion. Although solubilization is a popular approach, physicochemical principles underlying solubilization with respect to the choice of detergent are poorly understood. To gain insight into membrane dipole potential change and solubilization, we monitored solubilization of the hippocampal serotonin$_{1A}$ receptor and measured membrane dipole potential by the dual-wavelength fluorescence ratiometric approach using di-8-ANEPPS.[145] Figure 6b shows change in dipole potential upon solubilization, against the corresponding value of ligand binding activity of the serotonin$_{1A}$ receptor. The plot suggests the interdependence between the dielectric environment of the membrane interior (followed using magnitude of dipole potential) and solubilization (measured by specific agonist binding). The characterization of the mechanism of solubilization could help to move membrane solubilization techniques from *an art* to a much more rational basis. A more comprehensive understanding of the physical chemistry (such as dipolar reorganization within the membrane) underlying solubilization could add valuable information in the process of membrane protein reconstitution and in preparation of membrane protein crystals for X-ray crystallographic studies.

MICELLAR DIPOLE POTENTIAL: A NOVEL TOOL FOR DETERMINATION OF CRITICAL MICELLE CONCENTRATION

Do other organized assemblies such as micelles have dipole potential? To address this question, we previously explored the process of micelle formation from monomers for a representative variety of detergents and extended the concept of dipole potential to micellar systems.[147,148] We showed that the micelle formation process (Figure 7a) is associated with profound dipolar rearrangement, monitored as a change in micellar dipole potential by the dual-wavelength ratiometric approach using di-8-ANEPPS (Figure 7b,c).[147] Although the term dipole potential is generally used in the context of lipid bilayer membranes,[2,44,63,149] the nonrandom arrangement of amphiphiles and water dipoles would also contribute to dipole potential in organized molecular assemblies such as micelles. The voltage-sensitive fluorescent probe di-8-ANEPPS responds to change in dipole potential in micelles as it does in membranes due to an electrochromic mechanism. In other words, the photophysical property of the probe is independent of the shape and size of the organized molecular assembly in which it is localized. We showed that the characteristic trend of change in *R*-value during micelle formation could be utilized to estimate the critical micelle concentration (CMC) for a variety of detergents.[147] Figure 7b,c shows the micellization process of a representative anionic (sodium dodecyl sulfate, SDS) and cationic (cetyltrimethylammonium bromide, CTAB) detergent monitored using dipole potential measurement. The *R*-value exhibited maximum sensitivity to detergent concentration in a narrow range of concentrations around the CMC of the respective detergent, indicating significant dipolar reorganization during micelle formation, followed by a plateau in the post-micellar regime. Importantly, the trend of change in *R*-value during micellization can be effectively analyzed for determining the CMC of the corresponding detergent. The literature values of CMC and the values obtained using this approach are in overall agreement which validates this novel approach of CMC measurement. This approach of using dipole potential to explore micellar properties represents an exciting possibility of novel ways to explore micellar assemblies.

Structural transitions such as shape change play an important role in cell physiology and development.[150,151] Change of shape

https://doi.org/10.1021/acs.jpcb.2c02476
J. Phys. Chem. B 2022, 126, 4415−4430

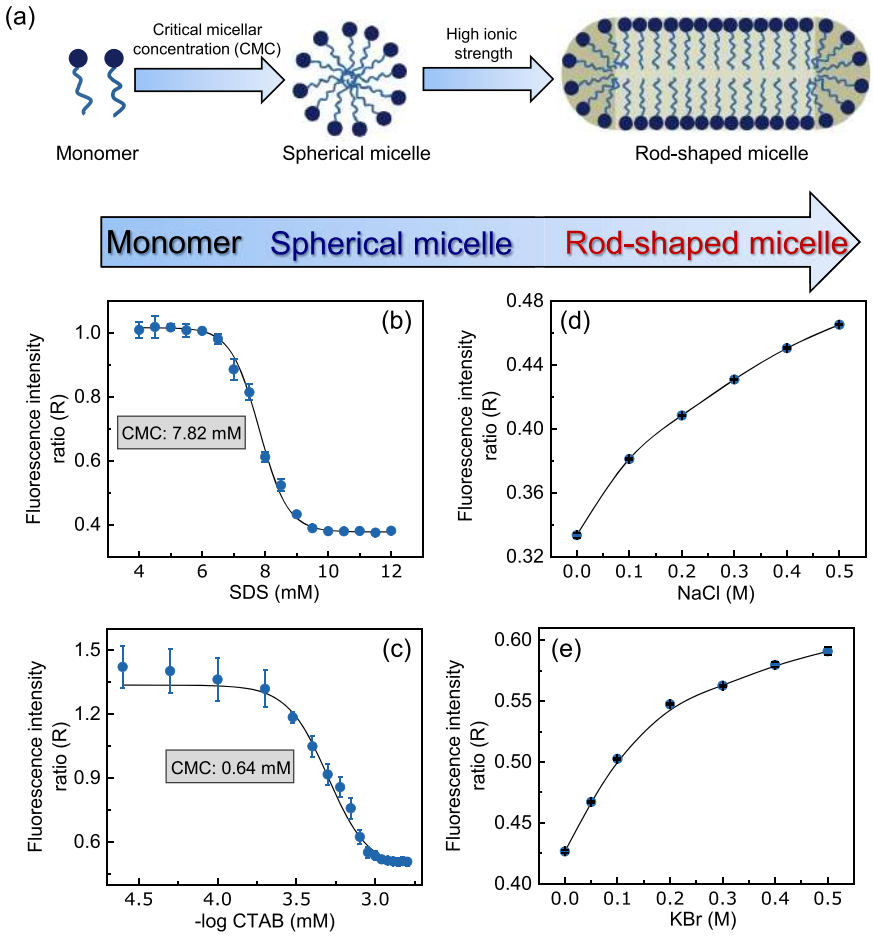

Figure 7. Dipole potential as a tool to monitor micellization. (a) A schematic representation of micelle formation from detergent monomers above the CMC and subsequently sphere-to-rod transition (in case of charged micelles) induced by high ionic strength. The structural transition takes place in charged micelles (such as SDS or CTAB) at concentrations well above the CMC. The microenvironment and packing of molecules in rod-shaped micelles are heterogeneous and are shown as cylindrical central part (lighter shade) and the spherical "end-caps" (darker shade). The headgroup spacing is reduced in the cylindrical part of the rod-shaped micelle due to attenuation of charge interactions by the added salt. The process of micellization for (b) SDS and (c) CTAB could be monitored using the change in the fluorescence intensity ratio (R) of the excitation spectra of di-8-ANEPPS with increasing detergent concentration. The curves in panels (b,c) are nonlinear regression fits to the experimental data. The calculated CMC values for each detergent are shown in each panel. Change in R of the excitation spectra of di-8-ANEPPS with increasing (d) NaCl concentration for SDS micelles and (e) KBr concentration for CTAB micelles are shown. Lines joining the data points are provided merely as viewing guides. Reprinted with permission from refs 147 and 148. Copyright 2015 Elsevier; see refs 147 and 148 for more details.

in cell membranes induced by an altered lipid composition is known to affect the function of membrane proteins such as mechanosensitive ion channels which are activated in response to changes in membrane curvature.[152] Charged micelles offer a suitable system in which structural transitions can be conveniently induced by modulating the ionic strength of the medium (Figure 7a).[153−158] We showed that sphere-to-rod structural transition in charged micelles of SDS and CTAB is associated with considerable dipolar reorganization (Figure 7d,e).[148] The micellar dipole potential exhibited an increase with increasing ionic strength (salt), due to an increase in the population of confined (nonrandom) dipoles induced by micellar shape change. It has been previously reported that selective removal of phospholipids from the outer membrane leaflet, alteration of membrane cholesterol level, metabolic depletion, and introduction of fatty acids and charged amphipathic agents in membranes lead to shape change of red blood cells.[159−161] It is envisioned that dipole potential measurements could provide novel insight into structural transitions in membranes that are associated with the dipolar reorganization.

VISUALIZING MEMBRANE DIPOLE POTENTIAL: INSIGHTS FROM DIPOLE POTENTIAL IMAGING

Modulation of membrane cholesterol content is utilized as a popular approach to assess the cholesterol-dependent function of membrane proteins and receptors. This is achieved by depletion of membrane cholesterol either in an acute[162,163] or chronic[75,164] fashion. For acute depletion, cholesterol is physically removed using carriers such as methyl-β-cyclodextrin (MβCD), a water-soluble carbohydrate polymer with a central nonpolar cavity that selectively and efficiently extracts cholesterol from membranes.[165,166] On the other hand, chronic (metabolic) depletion of cholesterol is typically achieved using inhibitors of cellular cholesterol biosynthetic pathway. For this, statins are used as a competitive inhibitor of HMG-CoA reductase, the rate-limiting key enzyme in the cholesterol biosynthetic pathway.[167] Importantly, statins are used extensively as cholesterol-lowering drugs to treat hypercholester-

https://doi.org/10.1021/acs.jpcb.2c02476
J. Phys. Chem. B 2022, 126, 4415−4430

olemia and dyslipidemia.[168] Cholesterol depletion using MβCD is an acute process due to the relatively short duration (~minutes) of treatment compared to a physiological scenario where cholesterol-lowering drugs (such as statins) take a longer time (hours to days) for cholesterol depletion. As a result, these two processes lead to different consequences in many cases (such as the organization of caveolae and GPI-anchored proteins,[169] induction of autophagy,[170] activity of sodium/phosphate cotransporter,[171] and endocytosis of GPCRs[172,173]), and this has resulted in a discussion on the fundamental differences underlying these processes. To address this issue, we measured the membrane dipole potential under conditions of acute and chronic cholesterol depletion in CHO-K1 cells, using a dual-wavelength ratiometric imaging approach (Figure 8).[174] This approach is relatively simple and straightforward to measure spatial variation in dipole potential of cell membranes from intact cells using commercially available fluorescence confocal microscopic setup.

For this, the surfaces of di-8-ANEPPS labeled CHO-K1 cells were imaged using two different excitation wavelengths (458 and 514 nm, corresponding to argon laser lines) with a 650−710 nm emission bandpass keeping all other parameters constant for both the images (see Figure 8a). Finally, a pixel-by-pixel map of the fluorescence intensity ratio (R), defined as the ratio of fluorescence intensities at an excitation wavelength of 458 nm to that at 514 nm (650−710 nm emission bandpass in both cases), was constructed. Although for fluorescence microscopy, an emission ratiometric method would have distinct advantages over excitation ratiometric method since it uses a single laser for excitation, the emission response of di-8-ANEPPS is not sensitive to the external electric field making emission ratiometric approach unsuitable.[49] However, for excitation ratiometric approach, one must correct for the difference in laser powers of two excitation wavelengths in order to compare the absolute R-values across different measurements. As mentioned earlier, the advantage of using di-8-ANEPPS is that it undergoes very slow internalization due to 2 octyl chains (instead of the butyl chains on di-4-ANEPPS).[29] As a result, the entire fluorescence of di-8-ANEPPS originates from the cell surface, and it can be used to follow dipole potentials over long time courses.[2,46,174] A representative example of dipole potential maps of cell membranes under chronic cholesterol-depleted conditions is shown in Figure 8a. As can be seen from the R-value heat map in Figure 8a, a progressive reduction in R is observed with increasing lovastatin concentration, that is, with decreasing membrane cholesterol. This is in overall agreement with earlier reports by us[44,140] and others[63] which showed cholesterol increases membrane dipole potential.[14] Further, to obtain a quantitative estimate of R, we averaged R over a large number of cells under both chronic and acute cholesterol depletion conditions. To gain insight into membrane dipole potential in response to cholesterol depletion under chronic and acute conditions, we plotted R as a function of membrane cholesterol content under these conditions (Figure 8b). The figure shows that R varies linearly with cholesterol content in both cases, although R was dependent more strongly on cholesterol content under chronic depletion conditions with a ~2-fold higher slope compared to when depletion was carried out acutely. This clearly suggests an intrinsic difference between these two processes of cholesterol depletion. When the highest concentration of lovastatin was used, ~87% of cholesterol was retained, corresponding to R of ~1.6 (Figure 8b). On the other hand, ~63% of cholesterol remained when cholesterol was

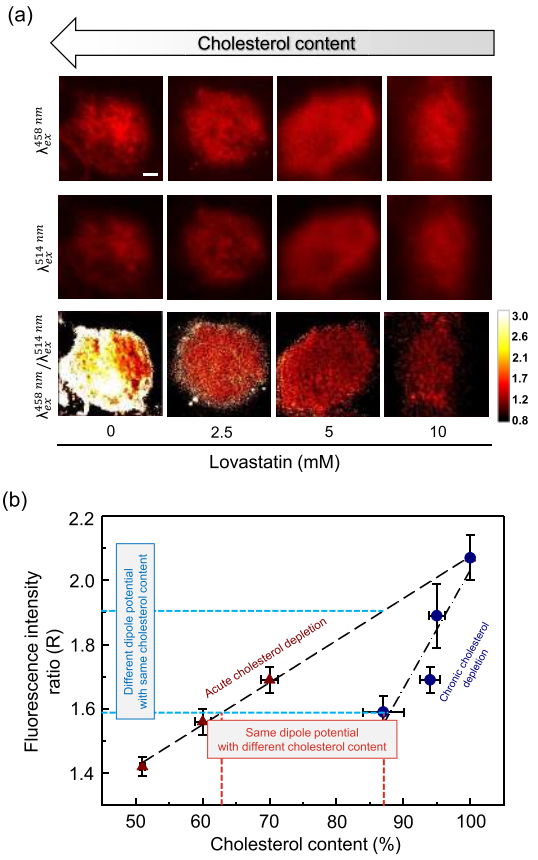

Figure 8. Dipole potential imaging reveals key molecular reorganization under acute and chronic cholesterol depletion conditions. (a) Representative confocal micrographs of CHO-K1 cells labeled with di-8-ANEPPS (λ_{ex} = 458 nm (upper panel) and λ_{ex} = 514 nm (middle panel); the emission bandpass was 650−710 nm in both cases) treated with increasing concentrations of lovastatin. The corresponding fluorescence intensity ratio (R) map (color-coded on a scale of 0.8−3) under these conditions is shown in the bottom panel. R is defined as the ratio of fluorescence intensities at an excitation wavelength of 458 nm to that at 514 nm (emission bandpass at 650−710 nm in both cases) and was calculated using ImageJ (NIH, Bethesda, MD). The color-coded map of R could be used to calculate membrane dipole potential averaged over multiple cells. (b) A plot of R (a measure of membrane dipole potential) with membrane cholesterol content for acute (MβCD; maroon triangle) and chronic (lovastatin; blue circle) depletion of cholesterol. An interesting feature is a difference in the slope observed under acute (~0.013) and chronic (~0.037) depletion conditions, thereby indicating a stronger dependence of R on cholesterol content under chronic depletion conditions. The orthogonal dotted projections on the axes show that membrane dipole potential could vary appreciably even when membrane cholesterol content is identical and vice versa. Reprinted with permission from ref 174. Copyright 2017 Springer Nature; see ref 174 for more details.

depleted acutely at the identical value of R (~1.6), thereby highlighting the key differences between the two methods. It is also apparent from the figure that membrane dipole potential exhibits differences under acute and chronic cholesterol depletion conditions, even when cholesterol content was identical. These results suggest that membrane dipole potential could reveal interesting differences in the reorganization of molecular dipoles within the membrane induced by acute and chronic cholesterol depletion, in addition to be dependent on membrane cholesterol content.[44,63,140] It should be noted that the membrane dipole potential would depend on the actual

https://doi.org/10.1021/acs.jpcb.2c02476
J. Phys. Chem. B 2022, 126, 4415−4430

process used to deplete cholesterol, and not *merely* on absolute membrane cholesterol content. Collective insight from this work could be relevant in understanding the ever-broadening functional role of membrane cholesterol in GPCR function. For example, we previously showed that the function[162,164] and oligomerization[175] of GPCRs such as the serotonin$_{1A}$ receptor exhibit a differential response to the actual process of cholesterol modulation. Insights highlighting the differences between various methods of cholesterol depletion could provide new avenues of understanding the role of cholesterol in cellular physiology associated with health and disease.

MODULATION OF DIPOLE POTENTIAL ACROSS THE CELL CYCLE

The cell cycle is a stringently regulated sequential multistep process essential for the growth and division of cells comprising multicellular organisms.[176] Although the involvement of nuclear and cytoplasmic proteins in cell cycle progression has been previously explored,[177] the role of lipids, membrane organization, and physical properties is a relatively unexplored area. We recently reported the modulation of membrane dipole potential in various stages of the cell cycle using the ratiometric imaging approach developed by us (Figure 9).[178] For measuring dipole potential in a cell cycle phase-specific manner, we utilized a flow cytometry-based approach to sort CHO-K1 cells into different cell cycle stages (G1, S, and G2/M) based on their DNA content. We subsequently carried out membrane dipole potential measurements using di-8-ANEPPS in these sorted cells that belong to specific cell cycle phases. Our results show that membrane dipole potential is highest in the G1 phase relative to S and G2/M phases (Figure 9a). In particular, dipole potential exhibited a significant reduction in S and G2/M phases (~10% and ~8%, respectively) relative to the G1 phase of the cell cycle. Interestingly, we observed a concomitant regulation of membrane cholesterol content in the cell cycle, with the highest cholesterol content in the G1 phase and considerable reduction in cholesterol in S and G2/M phases (Figure 9b). Most strikingly, we observed a close similarity in the dependence of membrane dipole potential and cholesterol with the progress of the cell cycle. Membrane dipole potential measurement therefore could be a sensitive tool for estimating transient physiological changes in lipid profile and conveniently used to monitor membrane physical properties in cellular systems. Interestingly, heterogeneity observed in the dipole potential in cell membranes has been correlated with the presence of lipid microdomains enriched in cholesterol and sphingolipids (often termed as "lipid rafts").[111,135,179,180] It has been reported, using three different ratiometric dipole potential sensitive probes and their colocalization with "lipid raft" markers (such as cholera toxin B, GPI-anchored green fluorescent protein, and an anticholesterol antibody) that the local dipole potential is significantly larger in lipid microdomains enriched in cholesterol than in the rest of the cell membrane.[135] This is further supported by observations made with atomic force microscopy performed with model membranes suggesting that the dipole potential is larger in liquid-ordered domains.[31]

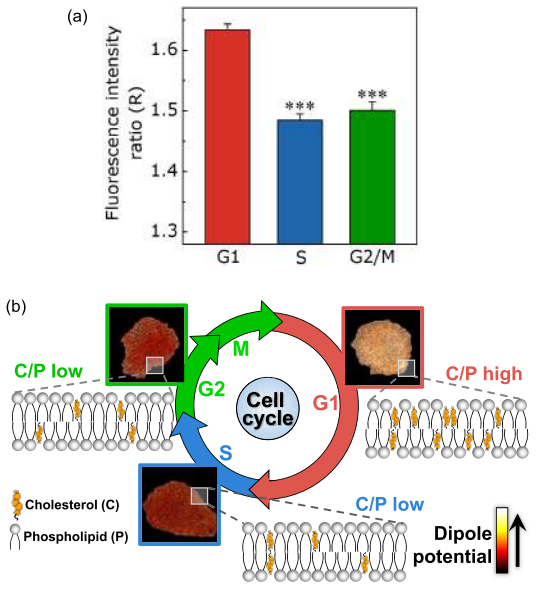

Figure 9. Cell cycle-dependent modulation of membrane dipole potential. (a) Modulation in *R*-value in specific stages of the cell cycle, averaged over ~40 independent measurements (*** corresponds to significant ($p < 0.001$) difference in *R* in S and G2/M phases of the cell cycle relative to G1 phase). Membrane dipole potential was measured in CHO-K1 cells by the ratiometric imaging approach described in Figure 8 using the voltage-sensitive probe di-8-ANEPPS. Membrane dipole potential is highest in the G1 phase relative to S and G2/M phases. (b) A schematic representation of concomitant regulation of membrane cholesterol content in the cell cycle, with highest cholesterol content in G1 phase and considerable reduction in cholesterol in S and G2/M phases. These suggest a close similarity in the dependence of membrane dipole potential and cholesterol with the progress of the cell cycle. C/P ratio refers to total cholesterol/total phospholipid ratio (mol/mol). Adapted with permission from ref 178. Copyright 2020 American Chemical Society; see ref 178 for more details.

Alterations in the lipid composition of the cell membrane are often associated with various diseases.[181] Cholesterol levels were previously shown to be modulated in cancer cells where cell cycle regulation was compromised.[182] Gaucher's disease is a lysosomal storage disorder that is characterized by the accumulation of glucosylceramide due to mutations in the enzyme glucocerebrosidase.[183] Importantly, sphingolipid accumulation, a characteristic of Gaucher's disease, significantly increases the magnitude of membrane dipole potential in the cell membranes.[135,184] These results suggest that changes in the lipid composition due to pathological conditions could modulate dipole potential in living cells, which could play an important role in the pathophysiology of these diseases. We believe that exploring the basis of cellular events from a biophysical perspective such as measurement of membrane dipole potential would result in a deeper understanding of such processes and their regulation in relation to cellular function.

CONCLUSIONS AND FUTURE PERSPECTIVES

In this Feature Article, we provide a glimpse into the ever-broadening functional role of dipole potential in biological membranes. We further highlight the enormous (and largely untapped) impact of dipole potential in addressing contemporary problems in membrane biology, with the possibility of adapting dipole potential measurements in various systems. This has increased the reach of dipole potential measurements to cellular systems, wherein a number of exciting and relevant biological questions can be probed using the dipole potential imaging approach. Taken together, the range of problems explored by our group and others using the membrane dipole potential approach shows that subtle changes in membrane dipole potential could be crucial in understanding the effect of

https://doi.org/10.1021/acs.jpcb.2c02476
J. Phys. Chem. B 2022, 126, 4415−4430

modulation of membrane lipids and the interplay between membrane lipids and proteins in the spatiotemporally complex cellular milieu. We envision that membrane dipole potential could turn out to be a convenient tool in the complex interplay between membrane lipids and proteins and could provide novel insight in membrane organization and function.

AUTHOR INFORMATION

Corresponding Author

Amitabha Chattopadhyay − *CSIR-Centre for Cellular and Molecular Biology, Hyderabad 500 007, India*; Phone: +91-40-2719-2578; Email: amit@ccmb.res.in

Author

Parijat Sarkar − *CSIR-Centre for Cellular and Molecular Biology, Hyderabad 500 007, India*

Complete contact information is available at: https://pubs.acs.org/10.1021/acs.jpcb.2c02476

Notes

The authors declare no competing financial interest.

Biographies

Dr. Parijat Sarkar received his integrated B.S.−M.S. degree from the Indian Institute of Science Education and Research Kolkata with major in biological sciences. He earned his Ph.D. from the CSIR-Centre for Cellular and Molecular Biology, Hyderabad, India, based on his work on the interplay between membrane lipids, actin cytoskeleton, and GPCRs carried out in Prof. Chattopadhyay's laboratory. He is a recipient of the Shyama Prasad Mukherjee Fellowship, National Academy of Sciences India Young Scientist Platinum Jubilee award and Sun Pharma Science Scholar award. His major interest is in membrane organization, dynamics, and GPCR−cholesterol interactions using fluorescence-based approaches.

Prof. Amitabha Chattopadhyay received his B.S. with honors in chemistry from St. Xavier's College (Calcutta) and M.S. in chemistry from Indian Institute of Technology, Kanpur. He obtained his Ph.D. from the State University of New York at Stony Brook and was a Postdoctoral Fellow at the University of California, Davis. He subsequently joined the Centre for Cellular and Molecular Biology in Hyderabad, where he is currently a CSIR Bhatnagar Fellow. Prof. Chattopadhyay's work is focused on the role of membrane lipids in the function of G protein-coupled receptors and its implications in health and disease using experimental and simulation approaches. A translational extension of this work has been on the role of host membrane lipids on the entry of intracellular pathogens into host cells. In addition, his group pioneered the development and application of the wavelength-selective fluorescence approach as a novel tool to monitor organization and dynamics of probes and proteins in membranes and micelles. Prof. Chattopadhyay was awarded the prestigious TWAS (The World Academy of Sciences) prize, Shanti Swarup Bhatnagar award, and Ranbaxy research award. He is an elected Fellow of TWAS, Royal Society of Biology, Royal Society of Chemistry, and all Indian Academies of Science. He has served and continues to be on the editorial board of a large number of reputable journals.

ACKNOWLEDGMENTS

Work in A.C.'s laboratory was generously funded by Department of Biotechnology, government of India, Council of Scientific and Industrial Research, Indo-French Centre for the Promotion of Advanced Research, University of Melbourne (IRRTF grant), and Science & Engineering Research Board, Department of Science and Technology, government of India. A.C. gratefully acknowledges support from SERB Distinguished Fellowship and CSIR Bhatnagar Fellowship. P.S. was supported as a Senior Project Associate by a CSIR FBR grant to A.C. (MLP 0146). Some of the work described in this article was carried out by former members of A.C.'s research group whose contributions are gratefully acknowledged. We thank Dr. Bhagyashree Rao (The Francis Crick Institute, London), Dr. G. Aditya Kumar (University of Michigan Medical School), Dr. Sreetama Pal (Cornell University), and members of the Chattopadhyay laboratory for critically reading the manuscript.

REFERENCES

(1) Pal, S.; Chattopadhyay, A. What is so unique about biomembrane organization and dynamics? In *Membrane Organization and Dynamics*; Chattopadhyay, A., Ed.; Springer: Heidelberg, 2017; pp 1−9.

(2) Gross, E.; Bedlack, R. S., Jr; Loew, L. M. Dual-wavelength ratiometric fluorescence measurement of the membrane dipole potential. *Biophys. J.* **1994**, *67*, 208−216.

(3) Honig, B. H.; Hubbell, W. L.; Flewelling, R. F. Electrostatic interactions in membranes and proteins. *Annu. Rev. Biophys. Biophys. Chem.* **1986**, *15*, 163−193.

(4) Kadir, L. A.; Stacey, M.; Barrett-Jolley, R. Emerging roles of the membrane potential: action beyond the action potential. *Front. Physiol.* **2018**, *9*, 1661.

(5) Hille, B. *Ion channels of Excitable Membranes*, 3rd ed.; Sinauer, Sunderland, MA, 2001.

(6) McLaughlin, S. Electrostatic potentials at membrane-solution interfaces. *Curr. Top. Membr. Transp.* **1977**, *9*, 71−144.

(7) Brockman, H. Dipole potential of lipid membranes. *Chem. Phys. Lipids* **1994**, *73*, 57−79.

(8) Clarke, R. J. The dipole potential of phospholipid membranes and methods for its detection. *Adv. Colloid Interface Sci.* **2001**, *89*−*90*, 263−281.

(9) Wang, L. Measurements and implications of the membrane dipole potential. *Annu. Rev. Biochem.* **2012**, *81*, 615−635.

(10) Seelig, J.; Macdonald, P. M.; Scherer, P. G. Phospholipid head groups as sensors of electric charge in membranes. *Biochemistry* **1987**, *26*, 7535−7541.
(11) Gawrisch, K.; Ruston, D.; Zimmerberg, J.; Parsegian, V. A.; Rand, R. P.; Fuller, N. Membrane dipole potentials, hydration forces, and the ordering of water at membrane surfaces. *Biophys. J.* **1992**, *61*, 1213−1223.
(12) Peterson, U.; Mannock, D. A.; Lewis, R. N. A. H.; Pohl, P.; McElhaney, R. N.; Pohl, E. E. Origin of membrane dipole potential: contribution of the phospholipid fatty acid chains. *Chem. Phys. Lipids* **2002**, *117*, 19−27.
(13) Starke-Peterkovic, T.; Clarke, R. J. Effect of headgroup on the dipole potential of phospholipid vesicles. *Eur. Biophys. J.* **2009**, *39*, 103−110.
(14) Clarke, R. J. Effect of cholesterol on the dipole potential of lipid membranes. *Adv. Exp. Med. Biol.* **2019**, *1115*, 135−154.
(15) Zakany, F.; Szabo, M.; Batta, G.; Kárpáti, L.; Mándity, I. M.; Fülöp, P.; Varga, Z.; Panyi, G.; Nagy, P.; Kovacs, T. An ω-3, but not an ω-6 polyunsaturated fatty acid decreases membrane dipole potential and stimulates endo-lysosomal escape of penetratin. *Front. Cell. Dev. Biol.* **2021**, *9*, 647300.
(16) Liberman, E. A.; Topaly, V. P. Permeability of bimolecular phospholipid membranes for fat-soluble ions. *Biofizika* **1969**, *14*, 452−461.
(17) Hladky, S. B.; Haydon, D. A. Membrane conductance and surface potential. *Biochim. Biophys. Acta* **1973**, *318*, 464−468.
(18) Haydon, D. A.; Myers, V. B. Surface charge, surface dipoles and membrane conductance. *Biochim. Biophys. Acta* **1973**, *307*, 429−443.
(19) Latorre, R.; Hall, J. E. Dipole potential measurements in asymmetric membranes. *Nature* **1976**, *264*, 361−363.
(20) Wang, L.; Bose, P. S.; Sigworth, F. J. Using cryo-EM to measure the dipole potential of a lipid membrane. *Proc. Natl. Acad. Sci. U.S.A.* **2006**, *103*, 18528−18533.
(21) Loew, L. M.; Bonneville, G. W.; Surow, J. Charge shift optical probes of membrane potential. Theory. *Biochemistry* **1978**, *17*, 4065−4071.
(22) Loew, L. M.; Scully, S.; Simpson, L.; Waggoner, A. S. Evidence for a charge-shift electrochromic mechanism in a probe of membrane potential. *Nature* **1979**, *281*, 497−499.
(23) Loew, L. M.; Simpson, L. L. Charge-shift probes of membrane potential: a probable electrochromic mechanism for *p*-aminostyrylpyridinium probes on a hemispherical lipid bilayer. *Biophys. J.* **1981**, *34*, 353−365.
(24) Loew, L. M. Design and characterization of electrochromic membrane probes. *J. Biochem. Biophys. Meth.* **1982**, *6*, 243−260.
(25) Gross, D.; Loew, L. M. Fluorescent indicators of membrane potential: microspectrofluorometry and imaging. *Methods Cell Biol.* **1989**, *30*, 193−218.
(26) Montana, V.; Farkas, D. L.; Loew, L. M. Dual-wavelength ratiometric fluorescence measurements of membrane potential. *Biochemistry* **1989**, *28*, 4536−4539.
(27) Loew, L. M.; Cohen, L. B.; Dix, J.; Fluhler, E. N.; Montana, V.; Salama, G.; Wu, J. Y. A naphthyl analog of the aminostyryl pyridinium class of potentiometric membrane dyes shows consistent sensitivity in a variety of tissue, cell, and model membrane preparations. *J. Membr. Biol.* **1992**, *130*, 130.
(28) Loew, L. M. Characterization of potentiometric membrane dyes. In *Biomembrane Electrochemistry*; Blank, M., Vodyanoy, I.; Eds.; American Chemical Society: Washington, DC, 1994; Chapter 8, Vol. *235*, pp 151−173.
(29) Loew, L. M. Potentiometric dyes: imaging electrical activity of cell membranes. *Pure Appl. Chem.* **1996**, *68*, 1405−1409.
(30) Perkins, W. R.; Cafiso, D. S. Procedure using voltage-sensitive spin-labels to monitor dipole potential changes in phospholipid vesicles: the estimation of phloretin-induced conductance changes in vesicles. *J. Membr. Biol.* **1987**, *96*, 165−173.
(31) Yang, Y.; Mayer, K. M.; Wickremasinghe, N. S.; Hafner, J. H. Probing the lipid membrane dipole potential by atomic force microscopy. *Biophys. J.* **2008**, *95*, 5193−5199.
(32) Hidaka, Y.; Asami, K. Measurement of dipole potential in bilayer lipid membranes by dielectric spectroscopy. *J. Membr. Biol.* **2014**, *247*, 721−727.
(33) Hu, W.; Webb, L. J. Direct measurement of the membrane dipole field in bicelles using vibrational Stark effect spectroscopy. *J. Phys. Chem. Lett.* **2011**, *2*, 1925−1930.
(34) Shrestha, R.; Cardenas, A. E.; Elber, R.; Webb, L. J. measurement of the membrane dipole electric field in DMPC vesicles using vibrational shifts of *p*-cyanophenylalanine and molecular dynamics simulations. *J. Phys. Chem. B* **2015**, *119*, 2869−2876.
(35) Shrestha, R.; Anderson, C. M.; Cardenas, A. E.; Elber, R.; Webb, L. J. Direct measurement of the effect of cholesterol and 6-ketocholestanol on the membrane dipole electric field using vibrational Stark effect spectroscopy coupled with molecular dynamics simulations. *J. Phys. Chem. B* **2017**, *121*, 3424−3436.
(36) Zhan, H.; Lazaridis, T. Influence of the membrane dipole potential on peptide binding to lipid bilayers. *Biophys. Chem.* **2012**, *161*, 1−7.
(37) Dreyer, J.; Zhang, C.; Ippoliti, E.; Carloni, P. Role of the membrane dipole potential for proton transport in gramicidin A embedded in a DMPC bilayer. *J. Chem. Theory Comput.h* **2013**, *9*, 3826−3831.
(38) Falkovich, S. G.; Martinez-Seara, H.; Nesterenko, A. M.; Vattulainen, I.; Gurtovenko, A. A. What can we learn about cholesterol's transmembrane distribution based on cholesterol-induced changes in membrane dipole potential? *J. Phys. Chem. Lett.* **2016**, *7*, 4585−4590.
(39) Shen, H.; Deng, M.; Wu, Z.; Zhang, J.; Zhang, Y.; Gao, C.; Cen, C. Effect of cholesterol on membrane dipole potential: atomistic and coarse-grained molecular dynamics simulations. *J. Chem. Theory Comput.h* **2018**, *14*, 3780−3795.
(40) Oakes, V.; Domene, C. Stereospecific interactions of cholesterol in a model cell membrane: implications for the membrane dipole potential. *J. Membr. Biol.* **2018**, *251*, 507−519.
(41) Shahane, G.; Ding, W.; Palaiokostas, M.; Orsi, M. Physical properties of model biological lipid bilayers: insights from all-atom molecular dynamics simulations. *J. Mol. Model.* **2019**, *25*, 76.
(42) Yee, S. M.; Gillams, R. J.; McLain, S. E.; Lorenz, C. D. Effects of lipid heterogeneity on model human brain lipid membranes. *Soft Matter* **2021**, *17*, 126−135.
(43) Shen, H.; Wu, Z.; Zou, X. Interfacial water structure at zwitterionic membrane/water interface: the importance of interactions between water and lipid carbonyl groups. *ACS Omega* **2020**, *5*, 18080−18090.
(44) Haldar, S.; Kanaparthi, R. K.; Samanta, A.; Chattopadhyay, A. Differential effect of cholesterol and its biosynthetic precursors on membrane dipole potential. *Biophys. J.* **2012**, *102*, 1561−1569.
(45) Fluhler, E.; Burnham, V. G.; Loew, L. M. Spectra, membrane binding, and potentiometric responses of new charge shift probes. *Biochemistry* **1985**, *24*, 5749−5755.
(46) Bedlack, R. S., Jr.; Wei, M.; Loew, L. M. Localized membrane depolarizations and localized calcium influx during electric field-guided neurite growth. *Neuron* **1992**, *9*, 393−403.
(47) Chattopadhyay, A.; London, E. Parallax method for direct measurement of membrane penetration depth utilizing fluorescence quenching by spin labeled phospholipids. *Biochemistry* **1987**, *26*, 39−45.
(48) Le Goff, G.; Vitha, M. F.; Clarke, R. J. Orientational polarisability of lipid membrane surfaces. *Biochim. Biophys. Acta* **2007**, *1768*, 562−570.
(49) Vitha, M. F.; Clarke, R. J. Comparison of excitation and emission ratiometric fluorescence methods for quantifying the membrane dipole potential. *Biochim. Biophys. Acta* **2007**, *1768*, 107−114.
(50) Clarke, R. J.; Kane, D. J. Optical detection of membrane dipole potential: avoidance of fluidity and dye-induced effects. *Biochim. Biophys. Acta* **1997**, *1323*, 223−239.
(51) Starke-Peterkovic, T.; Turner, N.; Else, P. L.; Clarke, R. J. Electric field strength of membrane lipids from vertebrate species: membrane

https://doi.org/10.1021/acs.jpcb.2c02476
J. Phys. Chem. B 2022, 126, 4415−4430

lipid composition and Na^+-K^+-ATPase molecular activity. *Am. J. Physiol. Regul. Integr. Comp. Physiol.* **2005**, *288*, R663−R670.
(52) Clarke, R. J. Effect of lipid structure on the dipole potential of phosphatidylcholine bilayers. *Biochim. Biophys. Acta* **1997**, *1327*, 269−278.
(53) O'Shea, P. Membrane potentials and membrane probes. In *Chemical Biology*; Larijani, B., Rosser, C. A., Woscholski, R., Eds.; John Wiley, West Sussex, UK, 2006; Chapter 5, pp 67−84.
(54) Simons, K.; Ikonen, E. How cells handle cholesterol. *Science* **2000**, *290*, 1721−1726.
(55) Mouritsen, O. G.; Zuckermann, M. J. What's so special about cholesterol? *Lipids* **2004**, *39*, 1101−1113.
(56) Maxfield, F. R.; van Meer, G. Cholesterol, the central lipid of mammalian cells. *Curr. Opin. Cell Biol.* **2010**, *22*, 422−429.
(57) Kumar, G. A.; Chattopadhyay, A. Cholesterol: an evergreen molecule in biology. *Biomed. Spectrosc. Imaging* **2016**, *5*, S55−S66.
(58) Krause, M. R.; Regen, S. L. The structural role of cholesterol in cell membranes: from condensed bilayers to lipid rafts. *Acc. Chem. Res.* **2014**, *47*, 3512−3521.
(59) Simons, K.; Toomre, D. Lipid rafts and signal transduction. *Nat. Rev. Mol. Cell Biol.* **2000**, *1*, 31−39.
(60) Simon, S. A.; McIntosh, T. J.; Latorre, R. Influence of cholesterol on water penetration into bilayers. *Science* **1982**, *216*, 65−67.
(61) Subczynski, W. K.; Wisniewska, A.; Yin, J. J.; Hyde, J. S.; Kusumi, A. Hydrophobic barriers of lipid bilayer membranes formed by reduction of water penetration by alkyl chain unsaturation and cholesterol. *Biochemistry* **1994**, *33*, 7670−7681.
(62) Nezil, F. A.; Bloom, M. Combined influence of cholesterol and synthetic amphiphilic peptides upon bilayer thickness in model membranes. *Biophys. J.* **1992**, *61*, 1176−1183.
(63) Starke-Peterkovic, T.; Turner, N.; Vitha, M. F.; Waller, M. P.; Hibbs, D. E.; Clarke, R. J. Cholesterol effect on the dipole potential of lipid membranes. *Biophys. J.* **2006**, *90*, 4060−4070.
(64) Szabo, G. Dual mechanism for the action of cholesterol on membrane permeability. *Nature* **1974**, *252*, 47−49.
(65) McIntosh, T. J.; Magid, A. D.; Simon, S. A. Cholesterol modifies the short-range repulsive interactions between phosphatidylcholine membranes. *Biochemistry* **1989**, *28*, 17−25.
(66) de Matos, A. M.; Blázquez-Sánchez, M. T.; Sousa, C.; Oliveira, M. C.; de Almeida, R. F. M.; Rauter, A. P. C-Glucosylation as a tool for the prevention of PAINS-induced membrane dipole potential alterations. *Sci. Rep.* **2021**, *11*, 4443.
(67) Nes, W. D. Biosynthesis of cholesterol and other sterols. *Chem. Rev.* **2011**, *111*, 6423−6451.
(68) Brown, A. J.; Sharpe, L. J. Cholesterol synthesis. In *Biochemistry of Lipids, Lipoproteins and Membranes*; Ridgway, N. D., McLeod, R. S., Eds.; Elsevier: Amsterdam, 2016; pp 327−358.
(69) Mitsche, M. A.; McDonald, J. G.; Hobbs, H. H.; Cohen, J. C. Flux analysis of cholesterol biosynthesis *in vivo* reveals multiple tissue and cell-type specific pathways. *eLife* **2015**, *4*, No. e07999.
(70) Waterham, H. R. Defects of cholesterol biosynthesis. *FEBS Lett.* **2006**, *580*, 5442−5449.
(71) Porter, F. D.; Herman, G. E. Malformation syndromes caused by disorders of cholesterol synthesis. *J. Lipid Res.* **2011**, *52*, 6−34.
(72) Irons, M.; Elias, E. R.; Salen, G.; Tint, G. S.; Batta, A. K. Defective cholesterol biosynthesis in Smith-Lemli-Opitz syndrome. *Lancet* **1993**, *341*, 1414.
(73) Chattopadhyay, A.; Paila, Y. D. Lipid-protein interactions, regulation and dysfunction of brain cholesterol. *Biochem. Biophys. Res. Commun.* **2007**, *354*, 627−633.
(74) Witsch-Baumgartner, M. DHCR7 mutations causing the Smith-Lemli-Opitz syndrome. *Future Lipidol.* **2008**, *3*, 585−593.
(75) Sharma, A.; Kumar, G. A.; Chattopadhyay, A. Late endosomal/lysosomal accumulation of a neurotransmitter receptor in a cellular model of Smith-Lemli-Opitz syndrome. *Traffic* **2021**, *22*, 332−344.
(76) Bloch, K. E. Sterol structure and membrane function. *CRC Crit. Rev. Biochem.* **1983**, *14*, 47−92.
(77) Arora, A.; Raghuraman, H.; Chattopadhyay, A. Influence of cholesterol and ergosterol on membrane dynamics: a fluorescence approach. *Biochem. Biophys. Res. Commun.* **2004**, *318*, 920−926.
(78) Shrivastava, S.; Chattopadhyay, A. Influence of cholesterol and ergosterol on membrane dynamics using different fluorescent reporter probes. *Biochem. Biophys. Res. Commun.* **2007**, *356*, 705−710.
(79) Shrivastava, S.; Paila, Y. D.; Dutta, A.; Chattopadhyay, A. Differential effects of cholesterol and its immediate biosynthetic precursors on membrane organization. *Biochemistry* **2008**, *47*, 5668−5677.
(80) Róg, T.; Pasenkiewicz-Gierula, M.; Vattulainen, I.; Karttunen, M. Ordering effects of cholesterol and its analogues. *Biochim. Biophys. Acta* **2009**, *1788*, 97−121.
(81) Shrivastava, S.; Paila, Y. D.; Kombrabail, M.; Krishnamoorthy, G.; Chattopadhyay, A. Role of cholesterol and its immediate biosynthetic precursors in membrane dynamics and heterogeneity: implications for health and disease. *J. Phys. Chem. B* **2020**, *124*, 6312−6320.
(82) Serfis, A. B.; Brancato, S.; Fliesler, S. J. Comparative behavior of sterols in phosphatidylcholine-sterol monolayer films. *Biochim. Biophys. Acta* **2001**, *1511*, 341−348.
(83) Lee, A. G. How lipids affect the activities of integral membrane proteins. *Biochim. Biophys. Acta* **2004**, *1666*, 62−87.
(84) Epand, R. M. Cholesterol and the interaction of proteins with membrane domains. *Prog. Lipid Res.* **2006**, *45*, 279−294.
(85) Chattopadhyay, A.; Rao, B. D.; Jafurulla, M. Solubilization of G protein-coupled receptors: a convenient strategy to explore lipid-receptor interaction. *Methods Enzymol.* **2015**, *557*, 117−134.
(86) Jafurulla, M.; Chattopadhyay, A. Structural stringency of cholesterol for membrane protein function utilizing stereoisomers as novel tools: a review. *Methods Mol. Biol.* **2017**, *1583*, 21−39.
(87) Mickus, D. E.; Levitt, D. G.; Rychnovsky, S. D. Enantiomeric cholesterol as a probe of ion-channel structure. *J. Am. Chem. Soc.* **1992**, *114*, 359−360.
(88) Covey, D. F. *ent*-Steroids: novel tools for studies of signaling pathways. *Steroids* **2009**, *74*, 577−585.
(89) D'Avanzo, N.; Hyrc, K.; Enkvetchakul, D.; Covey, D. F.; Nichols, C. G. Enantioselective protein-sterol interactions mediate regulation of both prokaryotic and eukaryotic inward rectifier K^+ channels by cholesterol. *PLoS One* **2011**, *6*, e19393.
(90) Kristiana, I.; Luu, W.; Stevenson, J.; Cartland, S.; Jessup, W.; Belani, J. D.; Rychnovsky, S. D.; Brown, A. J. Cholesterol through the looking glass: ability of its enantiomer also to elicit homeostatic responses. *J. Biol. Chem.* **2012**, *287*, 33897−33904.
(91) Jafurulla, M.; Rao, B. D.; Sreedevi, S.; Ruysschaert, J.-M.; Covey, D. F.; Chattopadhyay, A. Stereospecific requirement of cholesterol in the function of the serotonin$_{1A}$ receptor. *Biochim. Biophys. Acta* **2014**, *1838*, 158−163.
(92) Mannock, D. A.; McIntosh, T. J.; Jiang, X.; Covey, D. F.; McElhaney, R. N. Effects of natural and enantiomeric cholesterol on the thermotropic phase behavior and structure of egg sphingomyelin bilayer membranes. *Biophys. J.* **2003**, *84*, 1038−1046.
(93) Westover, E. J.; Covey, D. F.; Brockman, H. L.; Brown, R. E.; Pike, L. J. Cholesterol depletion results in site-specific increases in epidermal growth factor receptor phosphorylation due to membrane level effects. Studies with cholesterol enantiomers. *J. Biol. Chem.* **2003**, *278*, 51125−51133.
(94) Westover, E. J.; Covey, D. F. The enantiomer of cholesterol. *J. Membr. Biol.* **2004**, *202*, 61−72.
(95) Murari, R.; Murari, M. P.; Baumann, W. J. Sterol orientations in phosphatidylcholine liposomes as determined by deuterium NMR. *Biochemistry* **1986**, *25*, 1062−1067.
(96) Cheetham, J. J.; Wachtel, E.; Bach, D.; Epand, R. M. Role of the stereochemistry of the hydroxyl group of cholesterol and the formation of nonbilayer structures in phosphatidylethanolamines. *Biochemistry* **1989**, *28*, 8928−8934.
(97) Bandari, S.; Chakraborty, H.; Covey, D. F.; Chattopadhyay, A. Membrane dipole potential is sensitive to cholesterol stereospecificity:

https://doi.org/10.1021/acs.jpcb.2c02476
J. Phys. Chem. B 2022, 126, 4415−4430

implications for receptor function. *Chem. Phys. Lipids* **2014**, *184*, 25−29.
(98) Xu, F.; Rychnovsky, S. D.; Belani, J. D.; Hobbs, H. H.; Cohen, J. C.; Rawson, R. B. Dual roles for cholesterol in mammalian cells. *Proc. Natl. Acad. Sci. U.S.A.* **2005**, *102*, 14551−14556.
(99) Esfahani, M.; Scerbo, L.; Devlin, T. M. A requirement for cholesterol and its structural features for a human macrophage-like cell line. *J. Cell. Biochem.* **1984**, *25*, 87−97.
(100) Pearlstein, R. A.; Dickson, C. J.; Hornak, V. Contributions of the membrane dipole potential to the function of voltage-gated cation channels and modulation by small molecule potentiators. *Biochim. Biophys. Acta* **2017**, *1859*, 177−194.
(101) Valenta, C.; Cladera, J.; O'Shea, P.; Hadgraft, J. Effect of phloretin on the percutaneous absorption of lignocaine across human skin. *J. Pharm. Sci.* **2001**, *90*, 485−492.
(102) Alakoskela, J-M. I.; Söderlund, T.; Holopainen, J. M.; Kinnunen, P. K. J. Dipole potential and head-group spacing are determinants for the membrane partitioning of pregnanolone. *Mol. Pharmacol.* **2004**, *66*, 161−168.
(103) Maggio, B. Modulation of phospholipase A_2 by electrostatic fields and dipole potential of glycosphingolipids in monolayers. *J. Lipid Res.* **1999**, *40*, 930−939.
(104) Rokitskaya, T. I.; Antonenko, Y. N.; Kotova, E. A. Effect of the dipole potential of a bilayer lipid membrane on gramicidin channel dissociation kinetics. *Biophys. J.* **1997**, *73*, 850−854.
(105) Rokitskaya, T. I.; Kotova, E. A.; Antonenko, Y. N. Membrane dipole potential modulates proton conductance through gramicidin channel: movement of negative ionic defects inside the channel. *Biophys. J.* **2002**, *82*, 865−873.
(106) Efimova, S. S.; Zakharova, A. A.; Schagina, L. V.; Ostroumova, O. S. Local anesthetics affect gramicidin A channels via membrane electrostatic potentials. *J. Membr. Biol.* **2016**, *249*, 781−787.
(107) Cladera, J.; Martin, I.; Ruysschaert, J. M.; O'Shea, P. Characterization of the sequence of interactions of the fusion domain of the simian immunodeficiency virus with membranes. Role of the membrane dipole potential. *J. Biol. Chem.* **1999**, *274*, 29951−29959.
(108) Kovacs, T.; Zakany, F.; Nagy, P. It takes more than two to Tango: complex, hierarchal, and membrane-modulated interactions in the regulation of receptor tyrosine kinases. *Cancers (Basel)* **2022**, *14*, 944.
(109) Cladera, J.; O'Shea, P. Intramembrane molecular dipoles affect the membrane insertion and folding of a model amphiphilic peptide. *Biophys. J.* **1998**, *74*, 2434−2442.
(110) Cladera, J.; O'Shea, P.; Hadgraft, J.; Valenta, C. Influence of molecular dipoles on human skin permeability: use of 6-ketocholestanol to enhance the transdermal delivery of bacitracin. *J. Pharm. Sci.* **2003**, *92*, 1018−1027.
(111) Asawakarn, T.; Cladera, J.; O'Shea, P. Effects of the membrane dipole potential on the interaction of saquinavir with phospholipid membranes and plasma membrane receptors of Caco-2 cells. *J. Biol. Chem.* **2001**, *276*, 38457−38463.
(112) Ostroumova, O. S.; Kaulin, Y. A.; Gurnev, P. A.; Schagina, L. V. Effect of agents modifying the membrane dipole potential on properties of syringomycin E channels. *Langmuir* **2007**, *23*, 6889−6892.
(113) Ostroumova, O. S.; Malev, V. V.; Bessonov, A. N.; Takemoto, J. Y.; Schagina, L. V. Altering the activity of syringomycin E via the membrane dipole potential. *Langmuir* **2008**, *24*, 2987−2991.
(114) Efimova, S. S.; Zakharova, A. A.; Ismagilov, A. A.; Schagina, L. V.; Malev, V. V.; Bashkirov, P. V.; Ostroumova, O. S. Lipid-mediated regulation of pore-forming activity of syringomycin E by thyroid hormones and xanthene dyes. *Biochim. Biophys. Acta* **2018**, *1860*, 691−699.
(115) Ostroumova, O. S.; Malev, V. V.; Ilin, M. G.; Schagina, L. V. Surfactin activity depends on the membrane dipole potential. *Langmuir* **2010**, *26*, 15092−15097.
(116) Kovács, T.; Batta, G.; Hajdu, T.; Szabó, Á.; Váradi, T.; Zákány, F.; Csomós, I.; Szöllösi, J.; Nagy, P. The dipole potential modifies the clustering and ligand binding affinity of ErbB Proteins and their signaling efficiency. *Sci. Rep.* **2016**, *6*, 35850.
(117) Luchian, T.; Mereuta, L. Phlorizin- and 6-ketocholestanol-mediated antagonistic modulation of alamethicin activity in phospholipid planar membranes. *Langmuir* **2006**, *22*, 8452−8457.
(118) Mereuta, L.; Asandei, A.; Luchian, T. Meet me on the other side: trans-bilayer modulation of a model voltage-gated ion channel activity by membrane electrostatics asymmetry. *PloS One* **2011**, *6*, e25276.
(119) Li, S.; Wu, L.; Zhu, M.; Cheng, X.; Jiang, X. Effect of dipole potential on the orientation of voltage-gated Alamethicin peptides regulated by chaotropic anions. *J. Electroanal. Chem.* **2022**, *904*, 115880.
(120) Buzón, V.; Cladera, J. Effect of cholesterol on the interaction of the HIV GP41 fusion peptide with model membranes. Importance of the membrane dipole potential. *Biochemistry* **2006**, *45*, 15768−15775.
(121) Efimova, S. S.; Schagina, L. V.; Ostroumova, O. S. Channel-forming activity of cecropins in lipid bilayers: effect of agents modifying the membrane dipole potential. *Langmuir* **2014**, *30*, 7884−7892.
(122) Davis, S.; Davis, B. M.; Richens, J. L.; Vere, K. A.; Petrov, P. G.; Winlove, C. P.; O'Shea, P. α-Tocopherols modify the membrane dipole potential leading to modulation of ligand binding by P-glycoprotein. *J. Lipid Res.* **2015**, *56*, 1543−1550.
(123) Voglino, L.; McIntosh, T. J.; Simon, S. A. Modulation of the binding of signal peptides to lipid bilayers by dipoles near the hydrocarbon-water interface. *Biochemistry* **1998**, *37*, 12241−12252.
(124) Batta, G.; Kárpáti, L.; Henrique, G. F.; Tóth, G.; Tarapcsák, S.; Kovács, T.; Zakany, F.; Mándity, I. M.; Nagy, P. Statin-boosted cellular uptake and endosomal escape of penetratin due to reduced membrane dipole potential. *Br. J. Pharmacol.* **2021**, *178*, 3667−3681.
(125) Chaudhuri, A.; Chattopadhyay, A. Lipid binding specificity of bovine α-lactalbumin: a multidimensional approach. *Biochim. Biophys. Acta* **2014**, *1838*, 2078−2086.
(126) Thombare, V. J.; Holden, J. A.; Pal, S.; Reynolds, E. C.; Chattopadhyay, A.; O'Brien-Simpson, N. M.; Hutton, C. A. Antimicrobial activity of simplified mimics of celogentin C. *Tetrahedron* **2018**, *74*, 1288−1293.
(127) Qin, Z.; Szabo, G.; Cafiso, D. S. Anesthetics reduce the magnitude of the membrane dipole potential. measurements in lipid vesicles using voltage-sensitive spin probes. *Biochemistry* **1995**, *34*, 5536−5543.
(128) Cafiso, D. S. Dipole potentials and spontaneous curvature: membrane properties that could mediate anesthesia. *Toxicol. Lett.* **1998**, *100−101*, 431−439.
(129) Högberg, C.-J.; Lyubartsev, A. P. Effect of local anesthetic lidocaine on electrostatic properties of a lipid bilayer. *Biophys. J.* **2008**, *94*, 525−531.
(130) Mojumdar, E. H.; Lyubartsev, A. P. Molecular dynamics simulations of local anesthetic articaine in a lipid bilayer. *Biophys. Chem.* **2010**, *153*, 27−35.
(131) Davis, B. M.; Brenton, J.; Davis, S.; Shamsher, E.; Sisa, C.; Grgic, L.; Cordeiro, M. F. Assessing anesthetic activity through modulation of the membrane dipole potential. *J. Lipid Res.* **2017**, *58*, 1962−1976.
(132) Rao, B. D.; Shrivastava, S.; Pal, S.; Chattopadhyay, A. Effect of local anesthetics on the organization and dynamics of hippocampal membranes: a fluorescence approach. *J. Phys. Chem. B* **2019**, *123*, 639−647.
(133) Shrivastava, S.; Ror, P.; Chattopadhyay, A. Effect of local anesthetics on dipole potential of different phase membranes: a fluorescence study. *J. Membr. Biol.* **2022**, *255*, 363−369, DOI: 10.1007/s00232-022-00240-2.
(134) O'Shea, P. Physical landscapes in biological membranes: physico-chemical terrains for spatio-temporal control of biomolecular interactions and behaviour. *Philos. Trans. R. Soc. A* **2005**, *363*, 575−588.
(135) Kovács, T.; Batta, G.; Zákány, F.; Szöllösi, J.; Nagy, P. The dipole potential correlates with lipid raft markers in the plasma membrane of living cells. *J. Lipid Res.* **2017**, *58*, 1681−1691.
(136) Pucadyil, T. J.; Kalipatnapu, S.; Chattopadhyay, A. The serotonin$_{1A}$ receptor: a representative member of the serotonin receptor family. *Cell. Mol. Neurobiol.* **2005**, *25*, 553−580.

(137) Müller, C. P.; Carey, R. J.; Huston, J. P.; De Souza Silva, M. A. Serotonin and psychostimulant addiction: focus on 5-HT_{1A}-receptors. *Prog. Neurobiol.* **2007**, *81*, 133−178.
(138) Sarkar, P.; Kumar, G. A.; Pal, S.; Chattopadhyay, A. Biophysics of serotonin and the serotonin$_{1A}$ receptor: fluorescence and dynamics. In *Serotonin: The Mediator that Spans Evolution*; Pilowsky, P., Ed.; Elsevier: Amsterdam, 2018; pp 3−22.
(139) Sarkar, P.; Mozumder, S.; Bej, A.; Mukherjee, S.; Sengupta, J.; Chattopadhyay, A. Structure, dynamics and lipid interactions of serotonin receptors: excitements and challenges. *Biophys. Rev.* **2021**, *13*, 101−122.
(140) Singh, P.; Haldar, S.; Chattopadhyay, A. Differential effect of sterols on dipole potential in hippocampal membranes: implications for receptor function. *Biochim. Biophys. Acta* **2013**, *1828*, 917−923.
(141) Saxena, R.; Shrivastava, S.; Chattopadhyay, A. Exploring the organization and dynamics of hippocampal membranes utilizing pyrene fluorescence. *J. Phys. Chem. B* **2008**, *112*, 12134−12138.
(142) Robinson, D.; Besley, N. A.; O'Shea, P.; Hirst, J. D. Water order profiles on phospholipid/cholesterol membrane bilayer surfaces. *J. Comput. Chem.* **2011**, *32*, 2613−2618.
(143) Oishi, K.; Zheng, B.; White, J. F.; Vogler, W. R.; Kuo, J. F. Inhibition of Na, K-ATPase and sodium pump by anticancer ether lipids and protein kinase C inhibitors ET-18-OCH_3 and BM 41.440. *Biochem. Biophys. Res. Commun.* **1988**, *157*, 1000−1006.
(144) Sarkar, P.; Chattopadhyay, A. Solubilization of the serotonin$_{1A}$ receptor monitored utilizing membrane dipole potential. *Chem. Phys. Lipids* **2017**, *209*, 54−60.
(145) Kalipatnapu, S.; Chattopadhyay, A. Membrane protein solubilization: recent advances and challenges in solubilization of serotonin$_{1A}$ receptors. *IUBMB Life* **2005**, *57*, 505−512.
(146) Duquesne, K.; Sturgis, J. N. Membrane protein solubilization. *Methods Mol. Biol.* **2010**, *601*, 205−217.
(147) Sarkar, P.; Chattopadhyay, A. Dipolar rearrangement during micellization explored using a potential-sensitive fluorescent probe. *Chem. Phys. Lipids* **2015**, *191*, 91−95.
(148) Sarkar, P.; Chattopadhyay, A. Micellar dipole potential is sensitive to sphere-to-rod transition. *Chem. Phys. Lipids* **2016**, *195*, 34−38.
(149) Richens, J. L.; Lane, J. S.; Bramble, J. P.; O'Shea, P. The electrical interplay between proteins and lipids in membranes. *Biochim. Biophys. Acta* **2015**, *1848*, 1828−1836.
(150) Paluch, E.; Heisenberg, C.-P. Biology and physics of cell shape changes in development. *Curr. Biol.* **2009**, *19*, R790−R799.
(151) Bozelli, J. C., Jr.; Epand, R. M. Membrane shape and the regulation of biological processes. *J. Mol. Biol.* **2020**, *432*, 5124−5136.
(152) Perozo, E.; Kloda, A.; Cortes, D. M.; Martinac, B. Physical principles underlying the transduction of bilayer deformation forces during mechanosensitive channel gating. *Nat. Struct. Biol.* **2002**, *9*, 696−703.
(153) Rawat, S. S.; Chattopadhyay, A. Structural transition in the micellar assembly: a fluorescence study. *J. Fluoresc.* **1999**, *9*, 233−244.
(154) Rawat, S. S.; Kelkar, D. A.; Chattopadhyay, A. Effect of structural transition of the host assembly on dynamics of an ion channel peptide: a fluorescence approach. *Biophys. J.* **2005**, *89*, 3049−3058.
(155) Geng, Y.; Romsted, L. S.; Froehner, S.; Zanette, D.; Magid, L. J.; Cuccovia, I. M.; Chaimovich, H. Origin of the sphere-to-rod transition in cationic micelles with aromatic counterions: specific ion hydration in the interfacial region matters. *Langmuir* **2005**, *21*, 562−568.
(156) Arora-Sharawat, A.; Chattopadhyay, A. Effect of structural transition of the host assembly on dynamics of a membrane-bound tryptophan analogue. *Biophys. Chem.* **2007**, *129*, 172−180.
(157) Chaudhuri, A.; Haldar, S.; Chattopadhyay, A. Organization and dynamics in micellar structural transition monitored by pyrene fluorescence. *Biochem. Biophys. Res. Commun.* **2009**, *390*, 728−732.
(158) Chaudhuri, A.; Haldar, S.; Chattopadhyay, A. Structural transition in micelles: novel insight into microenvironmental changes in polarity and dynamics. *Chem. Phys. Lipids* **2012**, *165*, 497−504.
(159) Kuypers, F. A.; Roelofsen, B.; Berendsen, W.; Op den Kamp, J. A. F.; van Deenen, L. L. M. Shape changes in human erythrocytes induced by replacement of the native phosphatidylcholine with species containing various fatty acids. *J. Cell Biol.* **1984**, *99*, 2260−2267.
(160) Gedde, M. M.; Huestis, W. H. Membrane potential and human erythrocyte shape. *Biophys. J.* **1997**, *72*, 1220−1233.
(161) Backman, L.; Jonasson, J. B.; Hörsted, P. Phosphoinositide metabolism and shape control in sheep red blood cells. *Mol. Membr. Biol.* **1998**, *15*, 27−32.
(162) Pucadyil, T. J.; Chattopadhyay, A. Cholesterol depletion induces dynamic confinement of the G-protein coupled serotonin$_{1A}$ receptor in the plasma membrane of living cells. *Biochim. Biophys. Acta* **2007**, *1768*, 655−668.
(163) Kumar, G. A.; Sarkar, P.; Stepniewski, T. M.; Jafurulla, M.; Singh, S. P.; Selent, J.; Chattopadhyay, A. A molecular sensor for cholesterol in the human serotonin$_{1A}$ receptor. *Sci. Adv.* **2021**, *7*, eabh2922.
(164) Shrivastava, S.; Pucadyil, T. J.; Paila, Y. D.; Ganguly, S.; Chattopadhyay, A. Chronic cholesterol depletion using statin impairs the function and dynamics of human serotonin$_{1A}$ receptors. *Biochemistry* **2010**, *49*, 5426−5435.
(165) Zidovetzki, R.; Levitan, I. Use of cyclodextrins to manipulate plasma membrane cholesterol content: evidence, misconceptions and control strategies. *Biochim. Biophys. Acta* **2007**, *1768*, 1311−1324.
(166) Mahammad, S.; Parmryd, I. Cholesterol depletion using methyl-β-cyclodextrin. *Methods Mol. Biol.* **2015**, *1232*, 91−102.
(167) Istvan, E. S.; Deisenhofer, J. Structural mechanism for statin inhibition of HMG-CoA reductase. *Science* **2001**, *292*, 1160−1164.
(168) Endo, A. A historical perspective on the discovery of statins. *Proc. Jpn. Acad. Ser. B Phys. Biol. Sci.* **2010**, *86*, 484−493.
(169) Ilangumaran, S.; Hoessli, D. C. Effects of cholesterol depletion by cyclodextrin on the sphingolipid microdomains of the plasma membrane. *Biochem. J.* **1998**, *335*, 433−440.
(170) Cheng, J.; Ohsaki, Y.; Tauchi-Sato, K.; Fujita, A.; Fujimoto, T. Cholesterol depletion induces autophagy. *Biochem. Biophys. Res. Commun.* **2006**, *351*, 246−252.
(171) Breusegem, S. Y.; Halaihel, N.; Inoue, M.; Zajicek, H.; Lederer, E.; Barry, N. P.; Sorribas, V.; Levi, M. Acute and chronic changes in cholesterol modulate Na-Pi cotransport activity in OK cells. *Am. J. Physiol. Renal Physiol.* **2005**, *289*, F154−F165.
(172) Kumar, G. A.; Chattopadhyay, A. Statin-induced chronic cholesterol depletion switches GPCR endocytosis and trafficking: insights from the serotonin$_{1A}$ receptor. *ACS Chem. Neurosci.* **2020**, *11*, 453−465.
(173) Kumar, G. A.; Chattopadhyay, A. Membrane cholesterol regulates endocytosis and trafficking of the serotonin$_{1A}$ receptor: insights from acute cholesterol depletion. *Biochim. Biophys. Acta* **2021**, *1866*, 158882.
(174) Sarkar, P.; Chakraborty, H.; Chattopadhyay, A. Differential membrane dipolar orientation induced by acute and chronic cholesterol depletion. *Sci. Rep.* **2017**, *7*, 4484.
(175) Paila, Y. D.; Kombrabail, M.; Krishnamoorthy, G.; Chattopadhyay, A. Oligomerization of the serotonin$_{1A}$ receptor in live cells: a time-resolved fluorescence anisotropy approach. *J. Phys. Chem. B* **2011**, *115*, 11439−11447.
(176) Harper, J. V.; Brooks, G. The mammalian cell cycle: an overview. *Methods Mol. Biol.* **2005**, *296*, 113−153.
(177) Barnum, K. J.; O'Connell, M. J. Cell cycle regulation by checkpoints. *Methods Mol. Biol.* **2014**, *1170*, 29−40.
(178) Sarkar, P.; Rao, B. D.; Chattopadhyay, A. Cell cycle dependent modulation of membrane dipole potential and neurotransmitter receptor activity: role of membrane cholesterol. *ACS Chem. Neurosci.* **2020**, *11*, 2890−2899.
(179) O'Shea, P. Intermolecular interactions with/within cell membranes and the trinity of membrane potentials: kinetics and imaging. *Biochem. Soc. Trans.* **2003**, *31*, 990−996.
(180) Duggan, J.; Jamal, G.; Tilley, M.; Davis, B.; McKenzie, G.; Vere, K.; Somekh, M. G.; O'Shea, P.; Harris, H. Functional imaging of microdomains in cell membranes. *Eur. Biophys. J.* **2008**, *37*, 1279−1289.

https://doi.org/10.1021/acs.jpcb.2c02476
J. Phys. Chem. B 2022, 126, 4415−4430

(181) Simons, K.; Ehehalt, R. Cholesterol, lipid rafts, and disease. *J. Clin. Invest.* **2002**, *110*, 597−603.
(182) Brown, A. J. Cholesterol, statins and cancer. *Clin. Exp. Pharmacol. Physiol.* **2007**, *34*, 135−141.
(183) Butters, T. D. Gaucher disease. *Curr. Opin. Chem. Biol.* **2007**, *11*, 412−418.
(184) Batta, G.; Hajdu, T.; Nagy, P. Characterization of the effect of sphingolipid accumulation on membrane compactness, dipole potential, and mobility of membrane components. *Methods Mol. Biol.* **2021**, *2187*, 283−301.

https://doi.org/10.1021/acs.jpcb.2c02476
J. Phys. Chem. B 2022, 126, 4415−4430